Device

Article

SmartSleeve: A sutureless, soft robotic epicardial device that enables switchable on-off drug delivery in response to epicardial ECG sensing

Graphical abstract

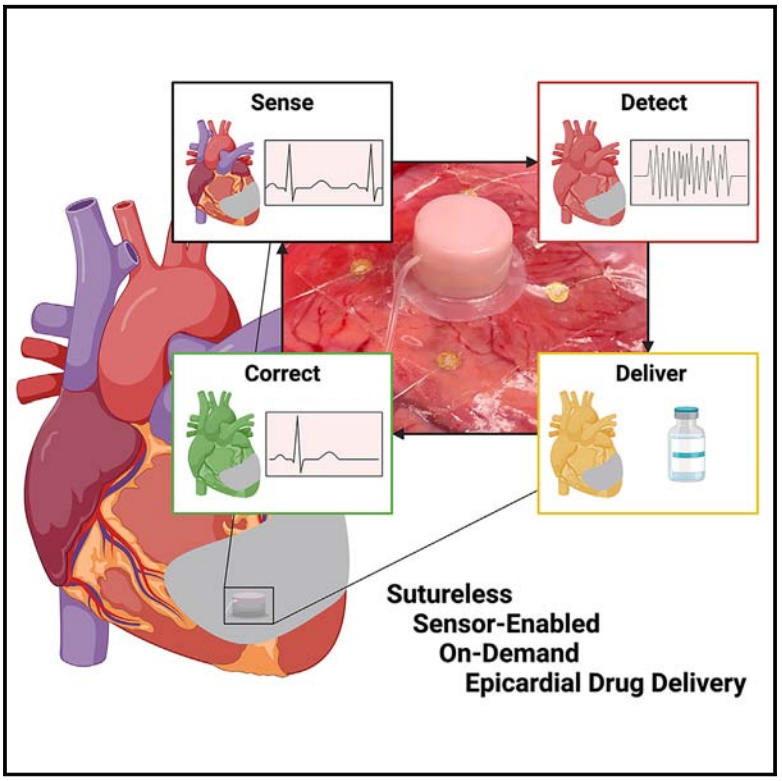

Authors

Keegan L. Mendez, Claudia E. Varela, Jean Bonnemain, ..., William Whyte, Xuanhe Zhao, Ellen T. Roche

Correspondence

etr@mit.edu

In brief

SmartSleeve is a sutureless, soft robotic drug-delivery device that enables switchable on-off drug delivery in response to epicardial ECG sensing. SmartSleeve allows for targeted epicardial drug delivery in response to real-time changes in the electrical activity of the heart, unlocking a new paradigm for "smart" cardiac therapy delivery. SmartSleeve offers the potential for accurate dosing and targeted delivery precisely when the patient needs it.

Highlights

- Highly tunable on-demand drug release from a soft robotic device
- Epicardial ECG sensing with a soft robotic device
- *In vivo* epicardial drug delivery in response to epicardial ECG sensing
- *In vitro* closed-loop drug delivery in response to real-time ECG signal

Develop
Prototype with demonstrated applications in relevant environment

Mendez et al., 2024, Device *2*, 100419
September 20, 2024 © 2024 The Authors. Published by Elsevier Inc.
https://doi.org/10.1016/j.device.2024.100419

CellPress

Please cite this article in press as: Mendez et al., SmartSleeve: A sutureless, soft robotic epicardial device that enables switchable on-off drug delivery in response to epicardial ECG sensing, Device (2024), https://doi.org/10.1016/j.device.2024.100419

Device

CellPress
OPEN ACCESS

Article

SmartSleeve: A sutureless, soft robotic epicardial device that enables switchable on-off drug delivery in response to epicardial ECG sensing

Keegan L. Mendez,[1,2] Claudia E. Varela,[1,2] Jean Bonnemain,[1,3] Jue Deng,[4] Hyunwoo Yuk,[4] Brian Ayers,[1,5] William Whyte,[1] Xuanhe Zhao,[4] and Ellen T. Roche[1,4,6,*]

[1]Institute for Medical Engineering and Science, Massachusetts Institute of Technology, Cambridge, MA 02139, USA
[2]Harvard-MIT Program in Health Sciences and Technology, Cambridge, MA 02139, USA
[3]Department of Adult Intensive Care Medicine, Lausanne University Hospital and University of Lausanne, Lausanne, Switzerland
[4]Department of Mechanical Engineering, Massachusetts Institute of Technology, Cambridge, MA 02139, USA
[5]Department of Surgery, Massachusetts General Hospital, Boston, MA 02114, USA
[6]Lead contact
*Correspondence: etr@mit.edu
https://doi.org/10.1016/j.device.2024.100419

THE BIGGER PICTURE Delivering drugs directly to the heart's surface holds promise for enhancing drug concentration at the intended site, mitigating systemic side effects, and reducing overall drug usage and expenses. However, the challenges associated with controllably targeting drugs to the epicardial surface have limited the exploration of epicardial delivery as a feasible route of administration. We introduce SmartSleeve, a sutureless, soft robotic drug-delivery device that enables precise, controlled drug delivery in response to electrocardiogram sensing at the epicardial surface. This innovative device offers a sophisticated platform to investigate localized drug delivery to the epicardium, with the potential to fundamentally change therapy delivery in clinical application such as postoperative arrhythmia management and long-term inotropic support.

SUMMARY

Epicardial drug delivery offers the potential to increase drug concentration at the target site, decrease systemic side effects, and reduce overall drug usage and cost. However, controlled drug delivery to the epicardium remains challenging, limiting exploration as a feasible administration route. Existing epicardial delivery systems lack precise control over drug dosing and responsiveness to local physiological cues. To address these limitations, we present SmartSleeve, a sutureless, soft robotic drug-delivery device that enables switchable on-off drug delivery in response to epicardial electrocardiogram (ECG) sensing. SmartSleeve is composed of an elastomeric soft robotic actuator with self-sealing therapy reservoirs, coupled to an adhesive bioelectronic interface. With SmartSleeve, we demonstrate controlled epicardial delivery of therapeutic agents in response to real-time ECG changes in animal models. SmartSleeve provides a sophisticated platform for studying epicardial drug delivery, with the potential to transform cardiac therapy delivery in clinical applications, including postoperative arrhythmia management and chronic inotropic support.

INTRODUCTION

Local epicardial drug delivery has appeal for several reasons, including increased drug concentration at the target tissue, decreased systemic side effects, and potentially reduced drug usage and cost. Epicardial drug delivery is currently understudied, however, due to the difficulty in locally targeting drugs to the epicardial surface in a controlled fashion. Current epicardial drug-delivery platforms utilize synthetic- or biomaterial-based patches loaded with the drug of interest.[1–6] These methods have some level of baseline drug release and a fixed drug-delivery profile, rendering them incapable of more sophisticated dosing regimes with on-off control or the ability to tune dosing once the device is deployed at the epicardial surface. Furthermore, these methods have no means of probing their local environment to provide feedback on physiological status or delivering drugs in response to local physiological signals.

Here, we present SmartSleeve, a soft robotic drug-delivery device capable of conformal adhesion to the epicardial surface, epicardial electrocardiogram (ECG) sensing, and on-demand

This is an open access article under the CC BY-NC-ND license (http://creativecommons.org/licenses/by-nc-nd/4.0/).

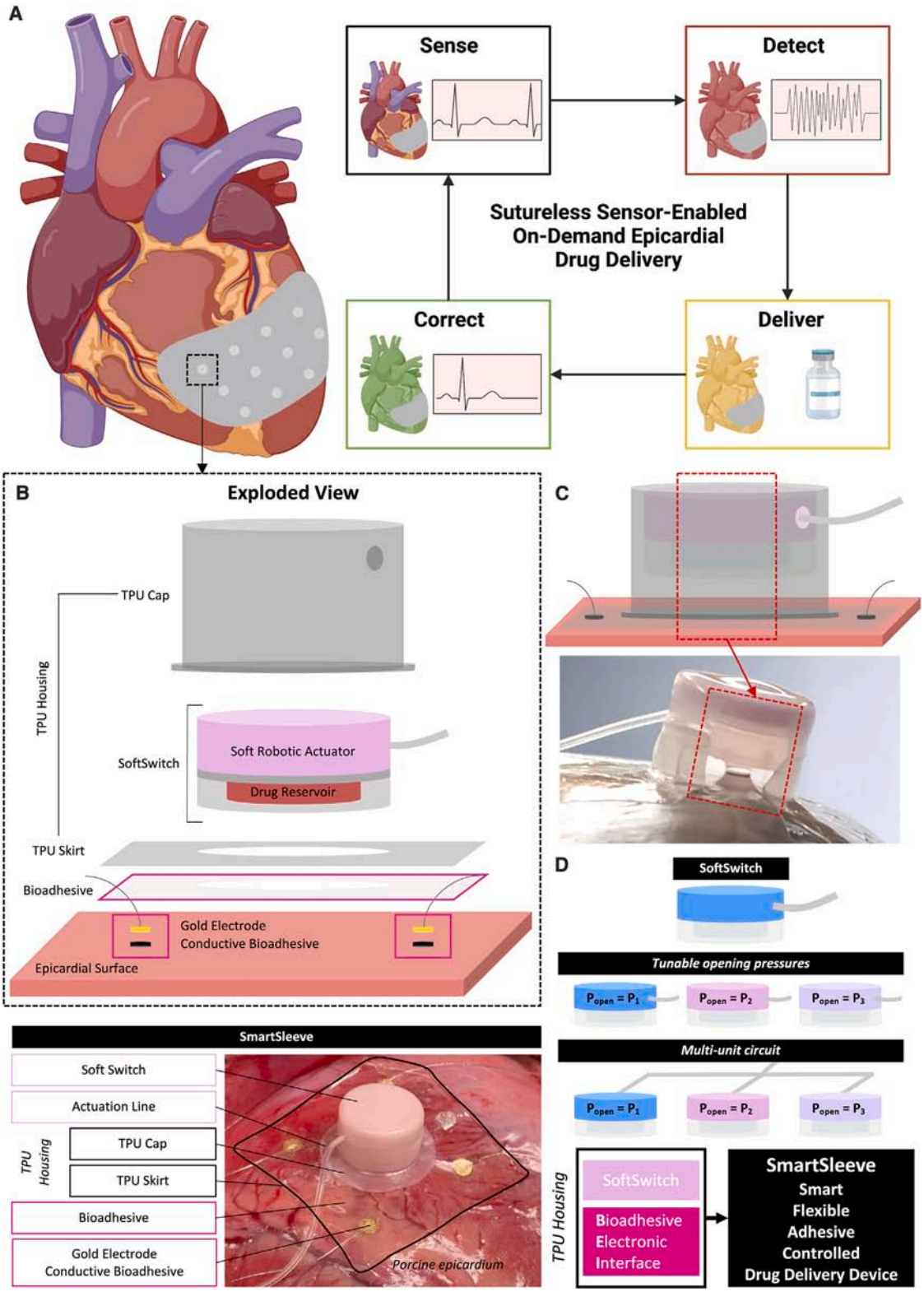

Figure 1. Overview of the SmartSleeve device and vision for controlled epicardial drug delivery

(A) SmartSleeve is a sutureless sensor-enabled soft robotic epicardial drug-delivery device. It is capable of conformal adhesion to the epicardial surface, epicardial ECG sensing, and on-demand epicardial drug delivery in response to the sensed ECG signal. In the future, SmartSleeve could be used to monitor ECG

(legend continued on next page)

Please cite this article in press as: Mendez et al., SmartSleeve: A sutureless, soft robotic epicardial device that enables switchable on-off drug delivery in response to epicardial ECG sensing, Device (2024), https://doi.org/10.1016/j.device.2024.100419

CellPress
OPEN ACCESS

epicardial drug delivery in response to the sensed ECG signal (Figure 1A). The ECG is an incredibly rich physiological signal that can be locally sensed at the epicardial surface and provide insight into pathophysiology.[7–9] SmartSleeve is composed of elastomeric soft robotic actuators with self-sealing drug reservoirs (one actuator per reservoir) coupled to an adhesive bioelectronic interface (Figure 1B). SmartSleeve enhances therapy delivery by allowing for sutureless, conformal adhesion to the epicardial surface, epicardial ECG sensing, and controlled, on-demand epicardial drug delivery with zero baseline drug release in response to the sensed ECG signal (Figure 1C). SmartSleeve offers a more sophisticated platform to better study local epicardial drug delivery and unlock a new paradigm for cardiac therapy delivery with potential for multiple clinical applications including localized drug delivery for patients who have failed systemic drug therapy and prior catheter ablation procedures, controlled drug delivery for modulation of the myocardial healing response post myocardial infarction, or in the rescue setting for detection and treatment of potentially lethal arrhythmias such as ventricular tachycardia.

RESULTS

Highly tunable on-demand drug release from a soft robotic device

The first step toward SmartSleeve realization is the development of a soft robotic drug-delivery platform that can be tuned to reliably deliver a predictable release profile on demand following a precise actuation regime. A single unit, consisting of a drug reservoir with a self-sealing silicone membrane coupled to an actuation chamber, is a SoftSwitch (Figures 1D and S1). Actuation above a pre-determined pressure threshold causes opening of the self-sealing pore, turning the device "ON" and allowing for drug release. The opening pressure threshold and the amount of drug released can be tuned and predicted based on the manufacturing and actuation parameters (Figure 1D). Tunable manufacturing parameters include elastomer stiffness, pore size, and membrane pre-stretch, and tunable actuation parameters include actuation rate, actuation volume, and number of actuation cycles. Multiple SoftSwitch units can also be combined to form a circuit (Figure 1D). SmartSleeve consists of a SoftSwitch housed in a functionalized epicardial sleeve that allows for sensor-enabled "smart" drug delivery (Figure 1D). Although we show a single SoftSwitch unit design of the SmartSleeve, it is a highly versatile platform that can be manufactured in a variety of shapes and configurations with multiple SoftSwitch units for a multi-reservoir sleeve.

SoftSwitch unit achieves on-off drug release

First, we developed a soft robotic drug-delivery device composed of an actuation layer and a sealed drug reservoir (Figure 2A). Application of a pneumatic stimulus above a pre-defined pressure threshold opens a self-sealing pore, turning the device "ON" and enabling localized drug release (Figure 2B). Subsequent pressure evacuation allows the pore to close and reseal, turning the device "OFF" (Figure 2B). The size and shape of the SoftSwitch platform are easily customizable because of the silicone molding manufacturing process (Figure S1). The platform can be manufactured in multiple sizes with varying drug-loading capabilities for deployment in different therapeutic applications in small and large animal models (Figure 2C).

We show that the self-sealing silicone membrane can achieve binary on-off control with zero baseline release while in the off configuration (Figure 2D). The device is considered "ON" when the actuation pressure is above the opening pressure. The device is considered "OFF" when the actuation pressure is below the opening pressure. Device activation is defined as actuation above the opening pressure (turning the device "ON") followed by evacuation below the opening pressure (turning the device "OFF"). To measure baseline release in the off configuration, devices were loaded with a model small-molecule drug (acid red 1) and submerged in release medium for 120 h. Devices exhibited negligible baseline release over this time interval ("OFF" configuration for $0 < t < 120$ h). To demonstrate binary on-off control, devices were activated on demand at $t = 120$ h ("ON" configuration at $t = 120$ h, immediately followed by "OFF" configuration for $t > 120$ h). Device activation resulted in rapid drug release while the device was "ON" ($t = 120$ h), followed by negligible baseline release after the device was turned back "OFF" ($t > 120$ h). Overall, these data demonstrate the ability for binary on-off control with zero undesired baseline release.

We show that we can modulate physiological pH using on-off delivery of two antagonizing agents *in vitro* (Figure 2E). Two switches loaded with a strong acid (HCl; switch A) and a strong base (NaOH; switch B) were submerged in water, and the pH was monitored in the surrounding fluid. Colorimetric change of a pH buffer was monitored for visual confirmation of pH change. The pH remained constant while the devices were in an "OFF" configuration ($0 < t <$ activate A). Activation of switch A containing an acid caused a drop in pH (switch A turned "ON" at $t =$ activate A), followed by maintenance of the lower pH while both devices were both off (activate A $< t <$ activate B). Activation of switch B containing a base subsequently restored the solution to near its baseline pH (switch B turned "ON" at $t =$ activate B), followed by maintenance of the baseline pH while both devices were again off ($t >$ activate B).

signals, detect a pathological ECG signal, deliver the appropriate therapy to address the pathological signal, and treat the pathological signal through continuous sensing, detection, delivery, and correction.

(B) SmartSleeve consists of a soft robotic drug-delivery device, SoftSwitch, composed of a soft robotic actuator and a self-sealing drug reservoir, that is coupled to a bioadhesive electronic interface (BEI) via a thermoplastic polyurethane (TPU) housing.

(C) Schematic (top) and *ex vivo* demonstration (bottom) of SmartSleeve coupled to epicardial surface. Bottom: triggering of SmartSleeve for controlled, on-demand, spatially targeted epicardial drug delivery.

(D) SoftSwitch is a single-reservoir soft robotic drug-delivery device that utilizes a self-sealing silicone pore. SoftSwitch can be manufactured to achieve tunable opening pressures and release profiles. Multiple SoftSwitch units can be combined into a multi-reservoir circuit to form multi-reservoir platforms with complex spatial and temporal delivery profiles. SmartSleeve consists of a SoftSwitch coupled to a flexible bioadhesive electronic interface via a TPU housing that allows for controlled, sensor-enabled "smart" drug delivery.

Please cite this article in press as: Mendez et al., SmartSleeve: A sutureless, soft robotic epicardial device that enables switchable on-off drug delivery in response to epicardial ECG sensing, Device (2024), https://doi.org/10.1016/j.device.2024.100419

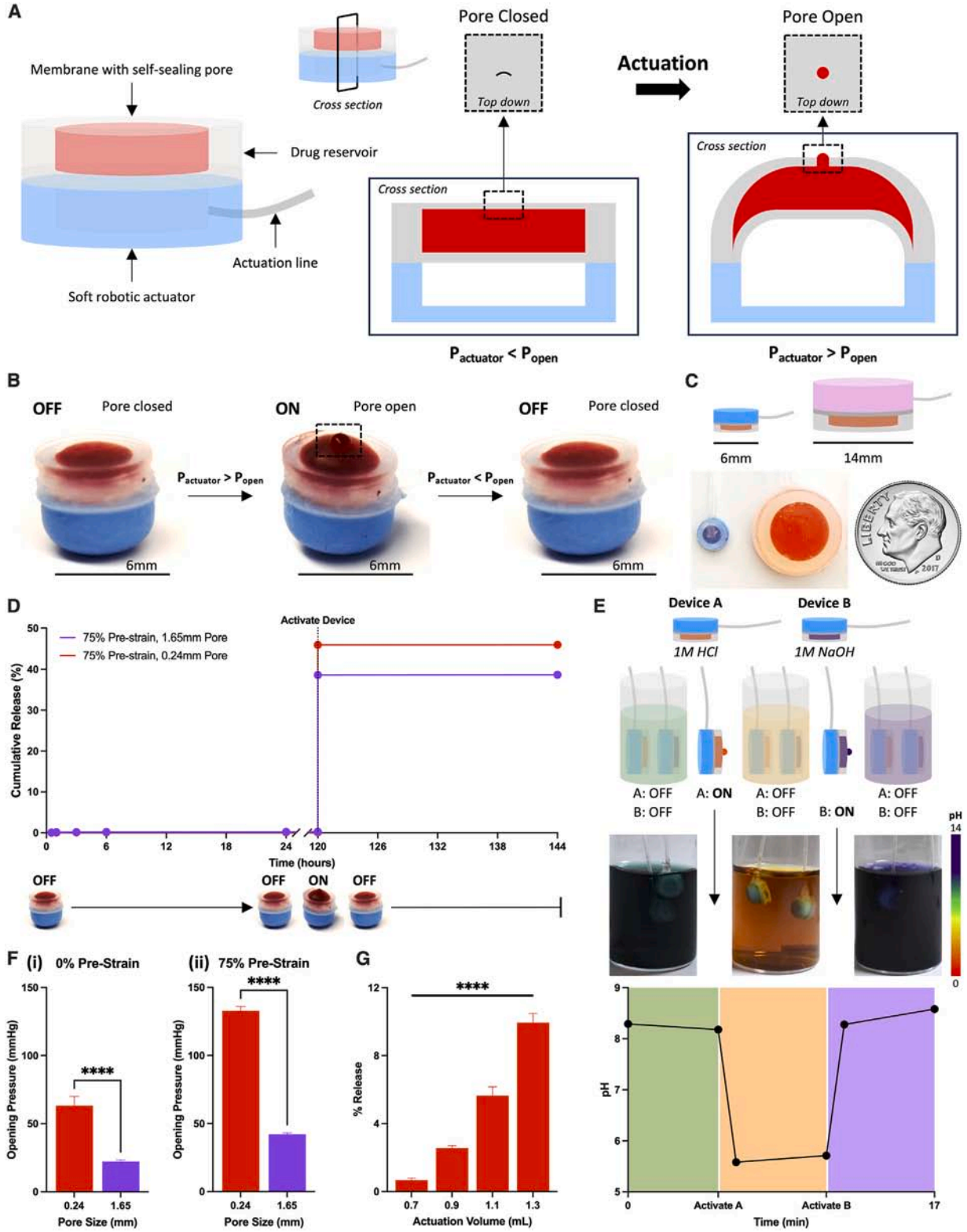

Figure 2. Design and realization of SoftSwitch, a milli-scale soft drug-delivery device

(A) Design schematic of SoftSwitch, a milli-scale soft drug-delivery device with switchable on-off control (left). An overview of the device mechanism of action is shown. The self-sealing pore remains closed when the device is at rest. The pore opens when the device is actuated (right).

(legend continued on next page)

Please cite this article in press as: Mendez et al., SmartSleeve: A sutureless, soft robotic epicardial device that enables switchable on-off drug delivery in response to epicardial ECG sensing, Device (2024), https://doi.org/10.1016/j.device.2024.100419

Next, we characterized the pressure upon which the device will switch to its "ON" configuration (i.e., opening of its self-sealing pore). We found that we can change the opening pressure by varying both the size of the needle used to make the self-sealing pore (Figure 2Fi) and the level of pre-strain of the silicone membrane while creating the pore (Figure 2Fii). Using a pressure gauge, we established an inverse relationship between the pore size and required opening pressure (Figure 2Fi). Opening pressure could be further modulated by pre-straining the silicone membrane before needle insertion (Figure 2Fii).

Finally, we demonstrated that we could tune the percentage of release from the device by varying the actuation volume during volume-controlled device actuation in a dose-responsive manner (Figure 2G). As we increased the actuation volume, we found an increasing level of release.

SoftSwitch unit can be tuned to predict drug release

After achieving on-off release, we aimed to further explore the tunability and predictability of the system. We developed a soft robotic drug-delivery device that can be more finely tuned to deliver drug over a spectrum of actuation regimes (Figure 3) with highly consistent drug-release profiles that can be predicted with a Gaussian process regression model leveraging six inputs to predict the percentage of drug release (Figure S8).

We created a library of switches (i.e., varying pore size and pre-strain conditions) (Figure 3Ai) and again characterized the pressure upon which the device will switch to its "ON" configuration (i.e., opening of its self-sealing pore) (Figure 3Aii). Again, we established an inverse relationship between pore size and opening pressure (Figure 3Bi–iii), showing that opening pressure decreases as pore size increases (Figures 3Bi–iii and S2). For each pore size, we demonstrated that opening pressure varies further with the degree of pre-stretch of the drug reservoir membrane (Figures 3Bi–iii and S2), showing that opening pressure increases as pre-stretch increases. Finally, we showed that opening pressure could also be modulated by varying the actuation rate (Figure 3Biv–vi), with opening pressure increasing with increasing actuation rate. We used the same library of switches to characterize the percent release, the percentage of drug delivered per actuation (Figure S3), where percent release is similarly dependent on pore size, membrane pre-stretch, and actuation rate. We found that for all actuation rates tested, percent release increases with increasing actuation volume (an indirect measure of pressure in volume-controlled actuation). For a given actuation volume, percent release decreases with increasing actuation rate. For a given actuation volume and actuation rate, percent release decreases with increasing pre-strain and increases with increasing pore size.

Multiple SoftSwitch units can be combined to enable controlled release of multiple agents

After the development and characterization of the SoftSwitch technology, we aimed to demonstrate that we could combine multiple switches to create a platform "circuit" that could be used for release of multiple agents with temporal and spatial control (Figure 4).

Four switches manufactured with four different switch conditions were loaded with colored fluids to represent four different drug proxies (Figure 4A). Switches were manufactured such that each switch had a different activation pressure. The four switches were then actuated in parallel via a single actuation line, with each of the four "drugs" released at a different location and time (Figure 4B). A Gaussian regression model was used to predict opening pressure based on manufacturing and actuation parameters of each switch. The four switches were activated sequentially as the actuation pressure increased, with each switch turning "ON" at its expected activation pressure (Figure 4B).

Integrating ECG sensing into a soft robotic device

After achieving highly tunable on-demand drug release, we set out to couple SoftSwitch units atraumatically to the epicardial surface and accurately sense the epicardial ECG signal. To this end, we developed a soft, thermoplastic polyurethane (TPU) housing that can be coupled with a previously reported[10] bioelectronic adhesive interface (BEI) via plasma treatment and a polyurethane (PU) layer (Figure S4). The TPU housing is made from TPU of discrete thicknesses thermally formed together. The thicker cap (0.305 mm) is designed to support the weight of the SoftSwitch device and maintain separation from the epicardial surface during device actuation. The lower thickness skirt (0.076 mm) is designed to maximize flexibility and conformal coupling with curved or uneven tissue surfaces. After the BEI is bonded to the TPU skirt via a polyurethane layer, the SoftSwitch device can be loaded into the housing. The fully integrated soft, sensor-enabled drug-delivery system, SmartSleeve, is then ready for adhesion to and electrical sensing at the epicardial surface (Figure 5).

Epicardial ECG sensing in a rodent model

We tested the ability for our fully integrated system to sense epicardial ECG in a rodent model (Figure 5A). We adhered our rodent-sized device (Figure 5Ai,ii) to the epicardial surface of a rat heart ($n = 8$) and recorded epicardial ECG (Figure 5Aiii). Simultaneously, we recorded surface ECG (Figure 5Aiv) by using conventional needle electrodes to evaluate the quality of the epicardial ECG signal and to monitor for possible arrhythmia generated by the device. We demonstrated successful recording of a stable epicardial ECG signal without any observable baseline shift or

(B) Demonstration of on-off drug release. The pore opens, and drug is released when the device is actuated at pressures above a pre-defined threshold, $P_{actuator}$.
(C) SoftSwitch devices at multiple length scales for use in small and large animal models. Small SoftSwitch (6 mm diameter; 13 μL reservoir volume) for use in a rat model (left). Large SoftSwitch (14 mm diameter; 400 μL reservoir volume) for use in a porcine model (right).
(D) Demonstration of on-off drug release with zero baseline release prior to device activation ($n = 3$ per group).
(E) Controlled modulation of pH after sequential activation and deactivation of multiple switches. Switch A contains strong acid (1 M HCl), and switch B contains strong base (1 M NaOH).
(F) Modulation of activation pressure by varying manufacturing parameters. Effect of pore size and pre-strain on device activation pressure ($n = 6$), mean ± SD. ****$p < 0.0001$, unpaired two-tailed t test with Welch's correction.
(G) Modulation of drug delivery by varying actuation regime. Effect of actuation volume on percent release ($n = 16$), mean ± SD. ****$p < 0.0001$, Welch's ANOVA test.

Please cite this article in press as: Mendez et al., SmartSleeve: A sutureless, soft robotic epicardial device that enables switchable on-off drug delivery in response to epicardial ECG sensing, Device (2024), https://doi.org/10.1016/j.device.2024.100419

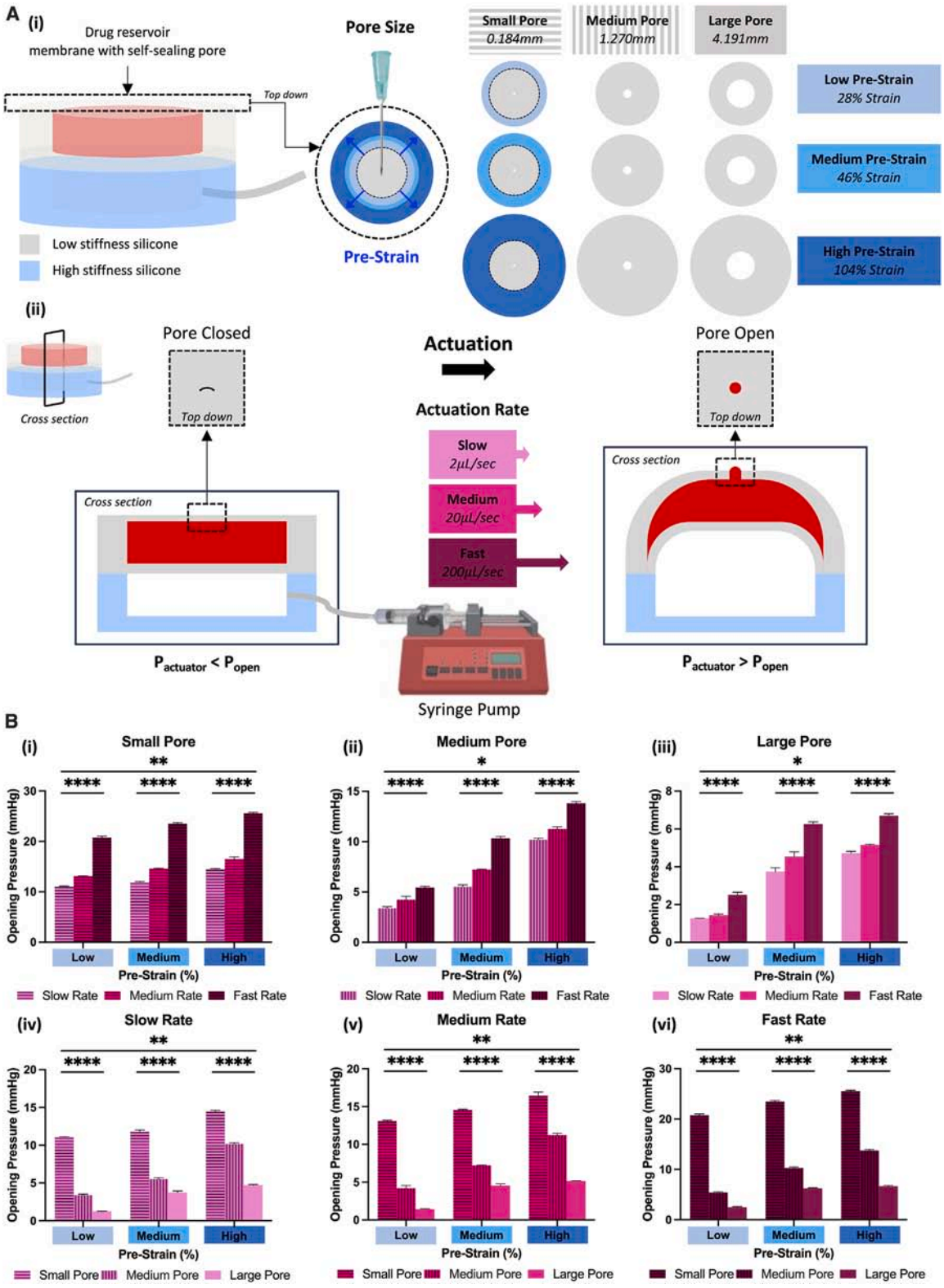

Figure 3. Tunable drug release from a soft robotic drug-delivery device

(A) (i) Manufacture of membranes at multiple pore sizes (small = 0.184 mm, medium = 1.270 mm, large = 4.191 mm) and levels of pre-strain (low = 28%, medium = 46%, high = 104%) to yield a library of switches. (ii) Actuation of switches at multiple rates (slow = 2 μL/s, medium = 20 μL/s, fast = 200 μL/s).

(legend continued on next page)

Please cite this article in press as: Mendez et al., SmartSleeve: A sutureless, soft robotic epicardial device that enables switchable on-off drug delivery in response to epicardial ECG sensing, Device (2024), https://doi.org/10.1016/j.device.2024.100419

high-amplitude noise. The surface ECG did not show any signs of arrhythmia. Next, we calculated the RR interval, the time elapsed between two successive R waves of the QRS signal (i.e., the reciprocal of heart rate), from both the epicardial and surface ECG signals (Figure 5Av). We found strong agreement between the RR intervals calculated from both signals, with near-zero difference between the epicardial and surface-derived RR intervals derived from the same cardiac cycle (Figure 5Avi).

Epicardial ECG sensing in a porcine model

Similarly, we tested the ability for our fully integrated system to sense epicardial ECG in a porcine model (Figure 5B). We adhered our porcine-sized device (Figure 5Bi,ii) to the epicardial surface of a porcine heart (n = 4) and recorded epicardial ECG (Figure 5Biii). We also recorded surface ECG (Figure 5Biv) using conventional methods to evaluate the quality of the epicardial ECG signal. We demonstrated successful recording of a stable epicardial ECG signal from the beating porcine heart without any observable baseline shift or high-amplitude noise. As in the rodent model, the surface ECG did not show any signs of arrhythmia caused by the device. We calculated the RR interval from both the epicardial and surface ECG signals and again found strong agreement between the RR intervals calculated from both signals (Figure 5Bv), with near-zero difference between the epicardial and surface-derived RR intervals derived from the same cardiac cycle (Figure 5Bvi).

SmartSleeve allows for controlled epicardial drug delivery in response to epicardial ECG sensing

After functionalizing our SoftSwitch technology with the BEI, we finally realize our goal of SmartSleeve. We demonstrate controlled epicardial drug delivery in response to epicardial ECG sensing *in vivo* enabled by robust and conformal adhesion to the epicardial surface, high-fidelity epicardial ECG sensing, and controllable on-off drug delivery.

Controlled epicardial drug delivery in a rodent model via SmartSleeve

We surgically implanted SmartSleeve on the epicardial surface in a rodent model (n = 8 rats) and tested the ability for sutureless epicardial adhesion, epicardial ECG sensing, and controllable release of an antiarrhythmic agent (amiodarone) (Figure 6A). We calculated RR interval, the time elapsed between successive R waves of the QRS signal, as a functional assessment of drug delivery. We expected RR interval to increase (decreased heart rate) following administration of amiodarone (Figure 6Ai). We used relative change (5% increase) in the RR interval and time to reach the relative change to determine whether drug had been successfully delivered and to measure the effects the epicardial drug delivery compared to systemic drug delivery. We compared the effect of epicardial delivery of amiodarone via device actuation (n = 3) to systemic delivery of amiodarone via tail-vein infusion (n = 8) (Figure 6Aii). We delivered the same dose of amiodarone (0.5 mg) at the epicardial surface or via tail-vein infusion and measured the time until a 5% relative increase in RR interval. We found a significant decrease in time to effect for device-enabled epicardial delivery. We demonstrated the ability for the device to deliver a controlled dose of amiodarone to the epicardial surface for faster, targeted drug delivery compared to systemic delivery in a single animal (Figure 6Aiii,iv). We saw no evidence of drug release prior to device actuation, demonstrating the ability for controlled, on-demand release (Figure 6Aiii,iv). Device-enabled epicardial delivery results in a larger physiological response than could be achieved by systemic delivery of the same dose (Figure S5).

Controlled epicardial drug delivery in a porcine model via SmartSleeve

We surgically implanted SmartSleeve on the epicardial surface in a porcine model (n = 3 swine) and tested the ability for sutureless epicardial adhesion, epicardial ECG sensing, and controllable release of a chronotropic agent (epinephrine) (Figure 6B). Again, we used RR interval as a functional assessment of drug delivery, expecting RR interval to decrease (increased heart rate) following administration of epinephrine (Figure 6Bi). We used relative changes in the RR interval to determine whether drug had been successfully delivered and to explore the effects of varying dose and delivery location. We compared the effect of epicardial delivery of two different epinephrine doses resulting from variations in device design and actuation regime. We delivered the two different doses of epinephrine (dose 1 = 4× dose 2) and measured the time until a 5% relative decrease in RR interval (Figure 6Bii). As expected, we found that a higher dose (Figure 6Biii) results in a more rapid "time to effect" than the lower dose (Figure 6Biv). We observed no evidence of drug release prior to device actuation, demonstrating the ability for controlled, on-demand release (Figure 6Biii,iv). Interestingly, we observed that the dose-adjusted relative change in RR interval was similar for both doses, although the higher dose reaches its maximum effect more rapidly (Figure S6).

Controlled epicardial drug delivery in response to epicardial ECG sensing via SmartSleeve

We validated complete SmartSleeve functionality in rodent and porcine models by demonstrating controlled epicardial drug delivery in response to epicardial ECG sensing (Figure 7). We demonstrated adhesion to the epicardial surface, high-fidelity epicardial ECG sensing, controlled drug delivery in response to a pre-determined ECG trigger signal, and confirmation of successful drug delivery via ECG sensing of a physiological change in response to the delivered drug.

In a rodent model, we demonstrated triggered amiodarone delivery following sensing of a 25% decrease in RR interval after intravenous (i.v.) administration of glycopyrrolate (Figure 7A). Glycopyrrolate was used to pharmacologically decrease the RR interval (increase heart rate) to serve as a trigger signal that could be sensed by the SmartSleeve device. The SmartSleeve device was set to activate following sensing of a 25% decrease in RR interval. We found that the SmartSleeve could sense the decrease in RR interval due to glycopyrrolate delivery and

(B) Effect of tunable membrane manufacturing, including pore size (i–iii), pre-strain, and actuation rate (iv–vi), on switch activation pressure (n = 3 devices per group; 5 activations per device), mean ± SD. (i) Small pore (0.184 mm); (ii) medium pore (1.270 mm); (iii) large pore (4.191 mm); (iv) slow rate (2 μL/s); (v) medium rate (20 μL/s); (vi) fast rate (200 μL/s). *p < 0.0332, **p < 0.0021, ***p < 0.0002, ****p < 0.0001, RM one-way ANOVA with Geisser-Greenhouse correction across pre-strain groups; ordinary one-way ANOVA with Tukey's multiple comparison test within each pre-strain group.

Please cite this article in press as: Mendez et al., SmartSleeve: A sutureless, soft robotic epicardial device that enables switchable on-off drug delivery in response to epicardial ECG sensing, Device (2024), https://doi.org/10.1016/j.device.2024.100419

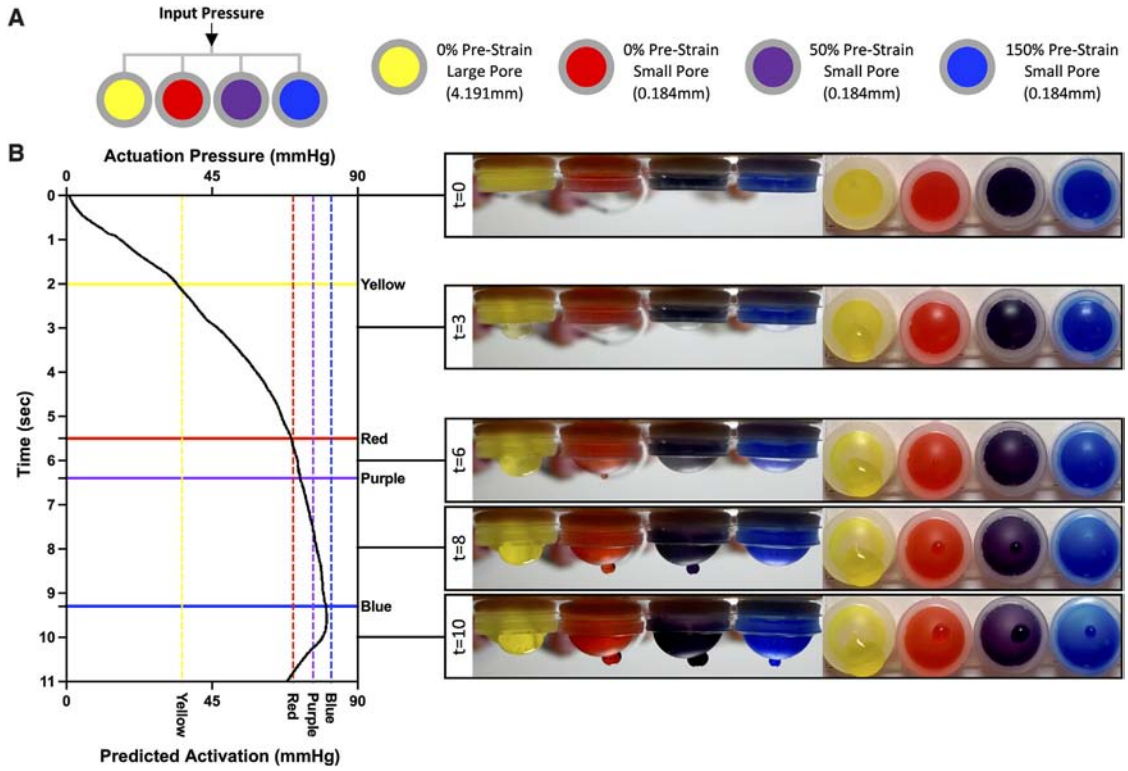

Figure 4. Spatial and temporal control of drug delivery via SoftCircuit, a soft robotic drug-delivery device with multiple SoftSwitch reservoirs

(A) Schematic of SoftCircuit, composed of four SoftSwitch devices manufactured with four different switch parameters, connected in parallel via a single actuation line.

(B) Actuation of SoftCircuit with serial activation of each switch as pressure is increased over time. Actuation pressure (black) during SoftCircuit actuation and serial activation of each switch. Solid horizontal lines indicate time of switch activation and subsequent drug release. Dashed horizontal lines indicate predicted activation pressure based on manufacturing parameters.

successfully deliver drug following sensing of the trigger signal (25% decrease in RR interval). The SmartSleeve could confirm successful drug delivery by sensing the increase in RR interval following device activation and amiodarone delivery.

In a porcine model, we demonstrated triggered epinephrine delivery following sensing of a return to baseline after pacing to 120 bpm (Figure 7B). The heart was externally paced to 120 bpm to decrease the RR interval (increase heart rate) to serve as a trigger signal that could be sensed by the SmartSleeve device. The SmartSleeve device was activated after sensing a return to baseline following termination of external pacing to 120 bpm. We demonstrate that the SmartSleeve could sense the decrease in RR interval due to pacing and successfully deliver drug following sensing of the trigger signal (pacing off and return to baseline). The SmartSleeve could confirm successful drug delivery by sensing the decrease in RR interval following device activation and epinephrine delivery.

Closed-loop control of drug delivery in response to real-time ECG signal

SmartSleeve can monitor changes in any part of the sensed ECG signal. The control system can measure and trigger off multiple time intervals, including RR, PR, QT, and QTc, and multiple amplitudes, such as P, Q, R, S, and T. The control system can also monitor and trigger off changes in unique user-defined variables that can be derived from the ECG—the system takes voltage as the input and can trigger actuation following any pre-determined "event criteria" that can be measured or calculated from the input voltage signal. Using a patient ECG simulator to generate a single-lead ECG signal (lead I) with varying heart rate, we demonstrate complete closed-loop control with the control system by sensing ECG, measuring RR interval, and automatically triggering device actuation each time the RR interval went below or above 0.8 s (Figure S7). We observe roughly a 2-s time delay between the threshold event and the actuation pulse, corresponding to signal processing and communication time between the data-acquisition system and the pneumatic control system (i.e., voltage signal read into PowerLab data-acquisition system, calculation of RR interval from voltage signal in LabChart software, recognition of trigger threshold in LabChart software, actuation pulse sent from PowerLab data-acquisition system to pneumatic control system). We believe that such a delay (~2 s) is reasonable within the clinical context of arrhythmia detection and treatment.

DISCUSSION

We present SmartSleeve, a sutureless, sensor-enabled, soft robotic epicardial drug-delivery device that enables switchable

Please cite this article in press as: Mendez et al., SmartSleeve: A sutureless, soft robotic epicardial device that enables switchable on-off drug delivery in response to epicardial ECG sensing, Device (2024), https://doi.org/10.1016/j.device.2024.100419

CellPress
OPEN ACCESS

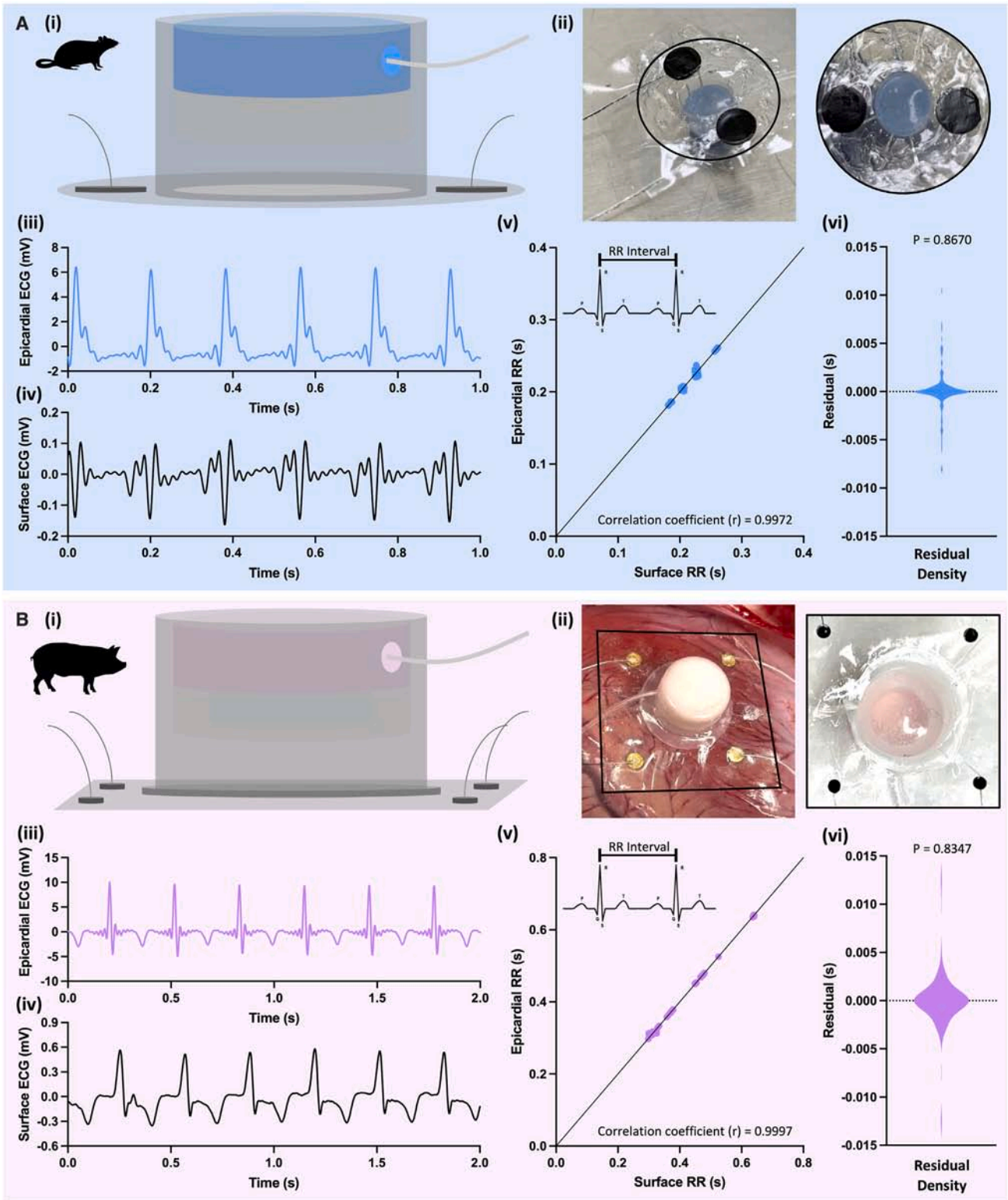

Figure 5. Epicardial ECG sensing in small and large animal models

(A) Design schematic (i) and realization (ii) of a rodent-sized soft robotic drug-delivery device that can be adhered to the epicardial surface and sense ECG signal. (iii and iv) Representative epicardial and surface ECG signals over the same cardiac cycles. (v) Comparison of RR interval measured from the epicardial and

(legend continued on next page)

Please cite this article in press as: Mendez et al., SmartSleeve: A sutureless, soft robotic epicardial device that enables switchable on-off drug delivery in response to epicardial ECG sensing, Device (2024), https://doi.org/10.1016/j.device.2024.100419

on-off drug delivery in response to epicardial ECG sensing. By coupling an elastomeric soft robotic actuator with a self-sealing drug reservoir to an adhesive bioelectronic interface, SmartSleeve is capable of sensor-enabled "smart" epicardial drug delivery that allows for localized epicardial therapy delivery with precise tunable spatial and temporal control, offering the potential for enhanced therapeutic efficacy while reducing off-target effects.

Initially, we demonstrated the design and realization of a soft robotic drug-delivery device (SoftSwitch) that utilizes a self-sealing silicone pore. We showed that we could achieve on-off drug release utilizing the self-sealing silicone pore (SoftSwitch). We could tune the opening pressure and release profile by varying the device manufacturing parameters, such as the size of the needle used to make the self-sealing pore or the level of pre-strain of the silicone membrane while creating the pore. For a given set of device manufacturing parameters, we could further tune the opening pressure and release profile by varying the device actuation parameters, including the actuation rate, the actuation volume, or the total number of actuation cycles. The technology and manufacturing workflow are highly versatile, enabling the use of any elastomer type, pore size, and level of pre-strain, with different permutations yielding different opening pressures and drug-release profiles. For any given device (i.e., specific combination of manufacturing parameters), the mechanism of pore opening, resulting in drug delivery, affords further tunability of drug release by varying the actuation regime (e.g., actuation rate or number of actuation cycles). A single SoftSwitch unit could be produced in different shapes and sizes, adding flexibility in terms of overall device dimensions and the total volume of drug that can be delivered, depending on the desired application. Multiple SoftSwitch devices could also be combined into multi-reservoir platforms, enabling spatial and temporal control of delivery of multiple therapeutic agents. Currently, the drug-delivery reservoir within a SoftSwitch unit is not refillable once deployed at the target site; however, our group has previously described multiple refillable systems for therapy delivery at the epicardial surface.[11,12] These systems leverage a second line to the therapy reservoir that can be used for therapy refills. In the future, the same mechanism could be incorporated into the current SoftSwitch design to enable therapy refill after use.

Next, we showed that we could combine the SoftSwitch platform technology with a conductive bioadhesive to enable epicardial adhesion and ECG sensing in rodent and porcine models. First, we showed that we could reliably sense epicardial ECG signal using the SmartSleeve device. We observed no significant differences in the ECG signal sensed with our device at the epicardial surface compared to the standard ECG signal measured with electrodes at the body surface. After validating sensing capabilities, we showed that we could use the SmartSleeve device for controlled epicardial drug delivery. We demonstrated on-demand epicardial drug delivery, with no evidence of undesired baseline drug release prior to device actuation. We explored the effects of route of administration (i.v. vs. epicardial) and dosing on both the time to effect and the magnitude of effect of drug delivery. For the tested drugs, we showed that we could use SmartSleeve to achieve both a faster time to effect and an increased magnitude of effect compared to the same dose administered intravenously. These results suggest that SmartSleeve can be used for targeted drug delivery, enabling usage of lower drug doses with faster response times. Targeted therapy has the potential to decrease the likelihood of toxicity and undesired off-target effects. Future work aims to utilize the control and tunability of this platform to delve deeper into the effects of varying drug dosing and site of administration on the level of physiological response and the time for the effect to manifest.

Finally, we exhibited validation of the fully functionalized SmartSleeve device in rodent and porcine models by demonstrating on-demand epicardial drug delivery in response to epicardial ECG sensing of a pre-determined trigger signal. In a rodent model, we used SmartSleeve for epicardial ECG sensing, sensing of the trigger signal, on-demand drug delivery after sensing the trigger signal, and confirmation of successful drug delivery as measured by the expected change in the ECG signal following drug action at the epicardial surface. We observed no evidence of undesired drug release prior to device actuation upon sensing of the trigger signal. Similarly, in a porcine model, we used SmartSleeve for epicardial ECG sensing, sensing of the trigger signal, on-demand drug delivery after sensing the trigger signal, and confirmation of successful drug delivery as measured by the expected change in the ECG signal following drug action at the epicardial surface. Again, we observed no evidence of unintentional drug release prior to triggered device actuation. In this work, we manually triggered device actuation after sensing the appropriate trigger signal *in vivo*. While not shown here, we have previously demonstrated automatically triggered actuation based on spirometry flow sensor data *in vivo* using the same control system.[13] To demonstrate that the control system can achieve complete closed-loop control of drug delivery in response to changes in ECG signal, we used a patient simulator to generate a time-varying ECG signal. The control system successfully sensed the ECG signal, monitored changes in RR interval, and automatically triggered device actuation, resulting in drug delivery each time the trigger signal was sensed. Future work aims to demonstrate complete closed-loop control of drug delivery *in vivo* in a porcine model.

Overall, we showed controlled epicardial drug delivery in response to epicardial ECG sensing *in vivo* enabled by robust and conformal device adhesion to the epicardial surface, high-fidelity epicardial ECG sensing, and controllable on-off drug delivery. SmartSleeve is a multi-functional platform technology with

surface ECG (n = 500 cycles from n = 8 rats). Correlation coefficient (r) = 0.9972. (vi) Residual density plot of paired t test between epicardial and surface-derived RR interval for the same cardiac cycle (n = 500 cycles from n = 8 rats). p = 0.8670; not statistically different, ns ($p > 0.1234$).

(B) Design schematic (i) and realization (ii) of a porcine-sized soft robotic drug-delivery device that can be adhered to the epicardial surface and sense ECG signal. (iii and iv) Representative epicardial and surface ECG signals over the same cardiac cycles. (v) Comparison of RR interval measured from the epicardial and surface ECG (n = 500 cycles from n = 4 pigs). r = 0.9997. (vi) Residual density plot of paired t test between epicardial and surface-derived RR interval for the same cardiac cycle (n = 500 cycles from n = 4 pigs). p = 0.8347; not statistically different, ns ($p > 0.1234$).

Please cite this article in press as: Mendez et al., SmartSleeve: A sutureless, soft robotic epicardial device that enables switchable on-off drug delivery in response to epicardial ECG sensing, Device (2024), https://doi.org/10.1016/j.device.2024.100419

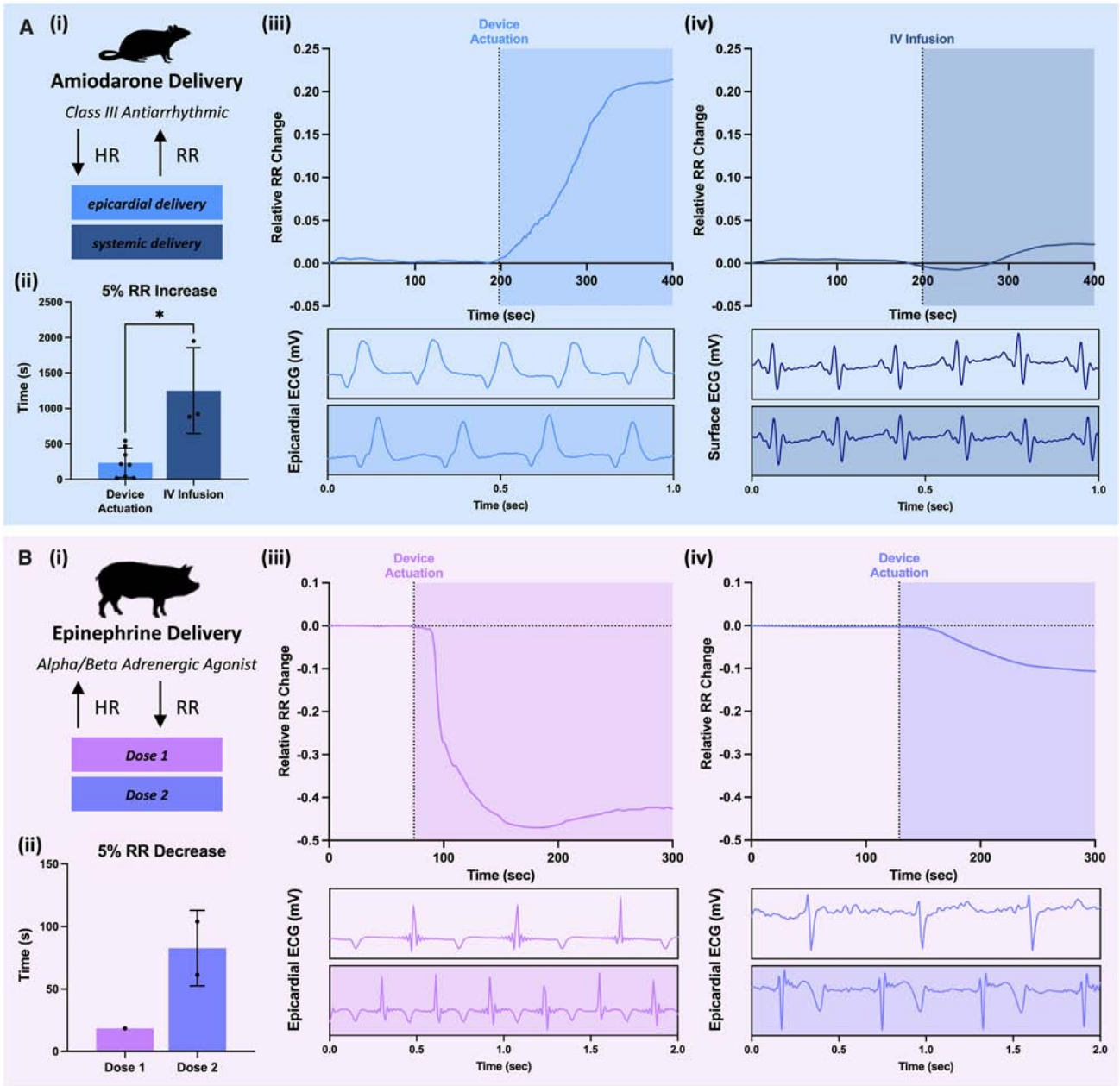

Figure 6. Controlled epicardial drug delivery from an adhesive sensing soft robotic device

(A) Amiodarone delivery in a rodent model. (i) Expected physiological changes following amiodarone delivery. (ii) Time for RR interval to increase by 5% following administration of the same dose of amiodarone via device actuation (epicardial delivery; $n = 7$) vs. i.v. infusion (systemic delivery; $n = 3$). (iii) Relative change in RR interval following device-enabled epicardial amiodarone delivery with representative epicardial ECG signals used to calculate RR interval before and after device actuation. (iv) Relative change in RR interval following i.v. infusion of amiodarone with representative surface ECG signals used to calculate RR interval before and after infusion.

(B) Epinephrine delivery in a porcine model. (i) Expected physiological changes following epinephrine delivery. (ii) Time for RR interval to decrease by 5% following device-enabled epicardial delivery of two different doses of epinephrine (dose 1 = 4× dose 2). (iii) Relative change in RR interval following device-enabled epicardial delivery of epinephrine dose 1 with representative epicardial ECG signals used to calculate RR interval before and after device actuation. (iv) Relative change in RR interval following device-enabled epicardial delivery of epinephrine dose 2 with representative epicardial ECG signals used to calculate RR interval before and after device actuation.

the ability to deliver multiple therapeutic agents in a dose-, time-, and spatially-controlled manner in response to electrical sensing. SmartSleeve can be manufactured in multiple shapes and sizes and can be adhered to wet and dynamic tissue surfaces without the use of sutures. In this work, we demonstrated SmartSleeve functionality and showed that it can be used to

Please cite this article in press as: Mendez et al., SmartSleeve: A sutureless, soft robotic epicardial device that enables switchable on-off drug delivery in response to epicardial ECG sensing, Device (2024), https://doi.org/10.1016/j.device.2024.100419

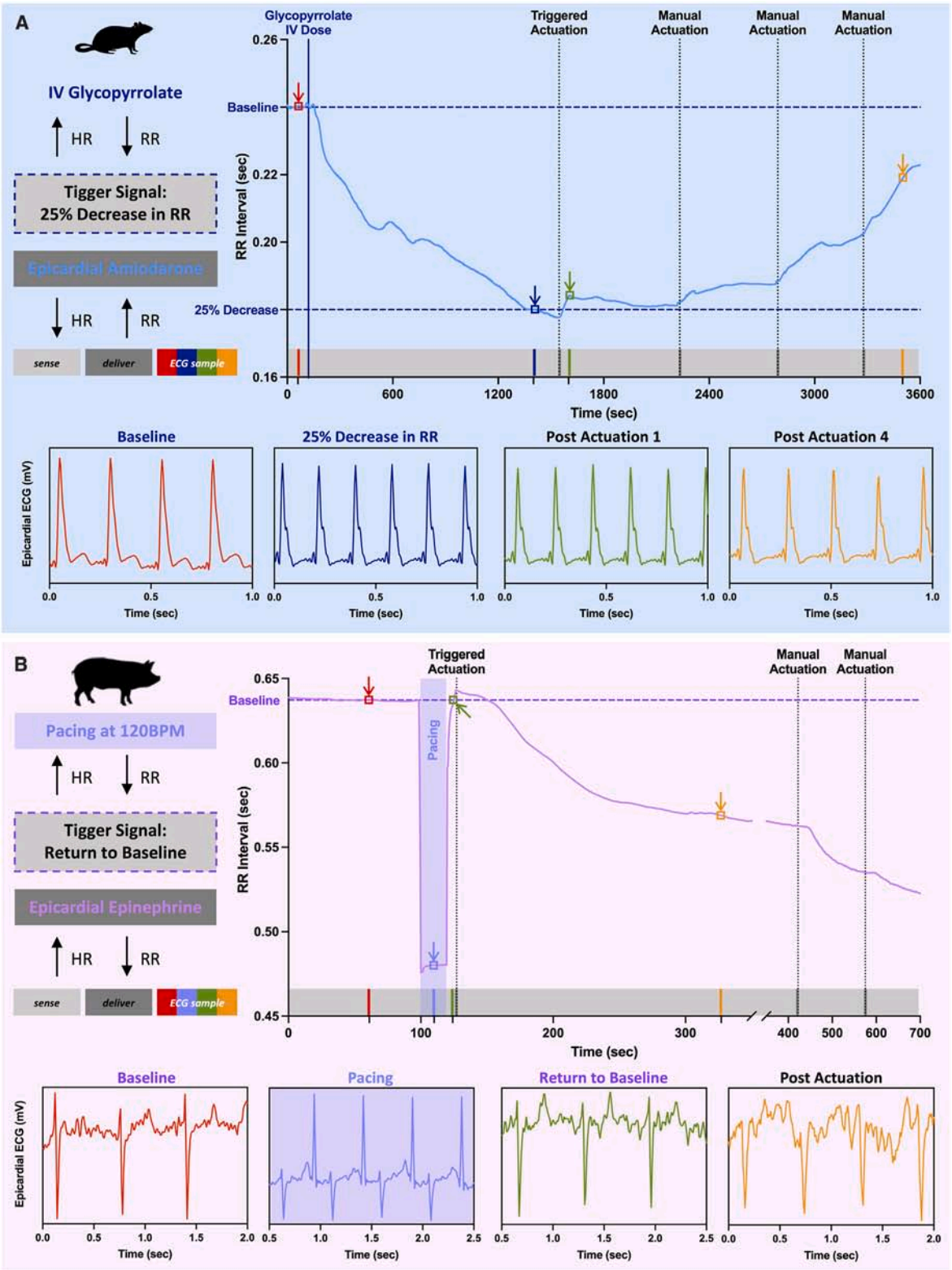

Figure 7. Controlled epicardial drug delivery in response to epicardial ECG sensing via SmartSleeve

(A) Epicardial amiodarone delivery in response to real-time epicardial ECG sensing in a rodent model. Device-enabled epicardial amiodarone delivery following sensing of a pre-determined trigger signal (25% decrease in RR interval from baseline). Intravenous administration of glycopyrrolate (expected to increase heart

(legend continued on next page)

Please cite this article in press as: Mendez et al., SmartSleeve: A sutureless, soft robotic epicardial device that enables switchable on-off drug delivery in response to epicardial ECG sensing, Device (2024), https://doi.org/10.1016/j.device.2024.100419

study epicardial delivery of multiple therapeutic agents in different animal models. SmartSleeve can serve as a powerful tool to better understand the pharmacokinetics of epicardial drug delivery and open the door to new dosing and delivery paradigms.

Looking forward, SmartSleeve could be deployed to detect and treat arrhythmias that are currently associated with a great degree of morbidity and mortality. While we recognize the numerous challenges between the proof-of-concept work presented here and this envisioned system, we suggest strategies below to enhance benefits and mitigate operative risk, aiming ultimately to improve patient outcomes and quality of life.

From the device standpoint, we acknowledge that SmartSleeve must be actuated via a pump that requires an energy supply. Our group is currently exploring opportunities for soft, implantable, fluidic-driven pumps that could be miniaturized and coupled with SmartSleeve for onboard actuation.[14] Energy could be supplied via transcutaneous energy transfer that is currently being developed for wireless powering of leadless pacemakers[15] and mechanical circulatory support systems (e.g., ventricular assist devices) to eliminate the need for drivelines.[16] ECG signal could be communicated wirelessly to an offboard external monitoring system like those used for implantable pacemakers and defibrillators.[17] This system could be monitored by a physician and communicate via Bluetooth with the onboard pump to trigger device actuation following sensing of the appropriate stimulus signal. Additionally, if the therapy reservoir were made refillable, it could be refilled via a subcutaneous port, like the access ports used in patients to deliver long-term chemotherapy.[18]

From the patient and procedural standpoint, well-defined criteria for patient selection and clinical indication would be essential to identify individuals who will derive the maximum benefit from this therapy. SmartSleeve could be especially useful in the postoperative setting where arrhythmias are common. The device would be implanted at the time of surgery, preventing the need for and risks associated with a separate procedure for implantation. Alternatively, SmartSleeve implantation could be justified in the outpatient setting for "difficult to treat" arrhythmias that have been refractory to systemic and procedural intervention. It would be necessary to offer the least invasive implantation approach that achieves a favorable risk-to-benefit ratio. In both clinical settings, it is critical to minimize the side effects of the antiarrhythmics, which may be achieved by smaller doses of locally administered medication through the SmartSleeve rather than non-specific systemic treatment.

SmartSleeve may also be useful clinically to deliver treatment that assists in myocardial wound healing after myocardial infarction. The localized delivery could open new opportunities to deliver medications that can modulate the inflammatory response and scar formation after myocardial infarction, potentially allowing patients to achieve a greater degree of recovery that would have a significant impact on their longevity and quality of life. Similarly, localized chronic inotropic support for congestive heart failure patients through SmartSleeve as either bridge to transplantation or palliative therapy could have a profound impact on patient lives by automating and simplifying the drug-delivery process. We recognize that surgery in patients suffering myocardial infarction or congestive heart failure can have high morbidity and mortality. As noted above, it would be necessary to offer the least invasive implantation approach that achieves a favorable risk-to-benefit ratio.

Along with the clinical advantages of controlled, localized, and automated drug delivery, we believe SmartSleeve could increase accessibility and equity by enabling out-of-hospital treatment and decreasing the burden of treatment for patients and caregivers alike. The SmartSleeve technology could also be deployed in non-cardiovascular clinical applications where sensing electrical signals, such as neural impulses, could be used to inform on-demand drug delivery. In summary, sensor-enabled control of drug delivery via SmartSleeve shows promise for enhancing epicardial drug delivery, enabling delivery of a precise dose of the correct cargo at the optimal time and location.

EXPERIMENTAL PROCEDURES

Resource availability

Lead contact

For additional information and resource requests, please contact Professor Ellen T. Roche at etr@mit.edu.

Materials availability

The study did not produce new unique reagents.

Data and code availability

The main article and supplemental information contain all the data presented in the study. Additional information can be requested from the corresponding author.

A soft implantable device that achieves on-off drug release

Manufacturing

A single-pour lost wax casting technique was used (Figure S1A). The actuation element was composed of high stiffness (Smooth-Sil 950) and low stiffness (Ecoflex 00-20) silicone to enable unidirectional actuation expansion. The self-sealing membrane (Ecoflex 00-20) was pre-stretched to varying strains (0%–75%) using a custom rig, and a pore was created using a hypodermic needle (0.24 mm or 1.65 mm) (Figure S1B). The membrane was then relaxed and bonded to the drug reservoir with a silicone adhesive (Sil-Poxy).

Activation pressure

Devices were actuated via volume-controlled actuation using a syringe pump (PhD Ultra, Harvard Apparatus) at a slow infusion rate (100 μL/min) while pressure was measured (ArgoTrans Model 2). A sudden drop in pressure (>2% in 1 s) indicated pore opening. This was confirmed by visual inspection.

rate and decrease RR interval) used to induce trigger signal for device actuation. Representative device-sensed epicardial ECG signal from baseline (red), following a 25% decrease in RR interval (blue), immediately following triggered device actuation (actuation 1; green), and following third manual device actuation (actuation 4; orange). Boxes with arrows on RR interval plot correspond to representative ECG signals used to calculate RR interval.

(B) Epicardial epinephrine delivery in response to real-time epicardial ECG sensing in a porcine model. Device-enabled epicardial epinephrine delivery following sensing of a pre-determined trigger signal (return to baseline following pacing to 120 bpm). External pacing (expected to increase heart rate and decrease RR interval) used to induce trigger signal for device actuation. Representative device-sensed epicardial ECG signal from baseline (red), during external pacing to 120 bpm (blue), immediately following return to baseline (green), and following triggered device actuation (actuation 1; orange). Boxes with arrows on RR interval plot correspond to representative ECG signals used to calculate RR interval.

Release measurement

Acid red 1 (10 mg/mL, Sigma 210633), HCl (1 M), or NaOH (1 M) were loaded into the device. Devices were submerged in water and actuated above their activation pressure (133 mmHg). Release was quantified by measuring absorbance at 506 nm (SpectraMax M3).

A soft implantable device that can be tuned to predict drug release

Manufacturing

The actuation element was composed of relatively high stiffness (Smooth-Sil 950) and low stiffness (Ecoflex 00-20) silicone to enable preferential expansion in one direction (Figure S1A). The self-sealing drug reservoir membrane (Ecoflex 00-20) was pre-stretched to varying strains (low, 28%; medium, 46%; high, 104%) using a custom rig, and a single pore was created using a hypodermic needle (small, 0.1842 mm; medium, 1.270 mm; large, 4.191 mm) (Figure S1B).

Activation pressure

To determine opening pressure, devices were actuated using a syringe pump (PhD Ultra, Harvard Apparatus) at a constant infusion rate (slow, 2 μL/s; medium, 20 μL/s; fast, 200 μL/s) while pressure was measured (Wireless Pressure Sensor, PASCO). A peak in pressure as determined by the "findpeaks" function in MATLAB indicated pore opening (MATLAB R2020b).

Release measurement

To determine drug release, devices were loaded with water and weighed with a high-precision scale. Devices were actuated as described previously and weighed following each actuation to determine volume loss with each opening.

Predictive model

To build a predictive model for drug-release profile, MATLAB Regression Learner toolbox was used to automatically assess a set of supervised machine-learning algorithms (Figure S8). Candidate regression models were trained and evaluated by applying 5-fold cross-validation, then ranked according to root-mean-squared error (RMSE). The top-performing model, a Gaussian process regressor (RMSE = 0.488; *R*-squared = 0.99; mean squared error [MSE] = 0.238; mean absolute error [MAE] = 0.190) was subsequently used to predict the output drug release (% release) as a function of the input device manufacturing parameters (pore size, membrane pre-strain, drug-loading volume) and device actuation parameters (actuation volume, actuation pressure, number of prior actuations). The RMSE of 0.4888 corresponds to an error of ~0.5% drug release. For the maximum drug-loading volume used in this work (400 μL), this represents an error in predicted drug release of up to 2 μL of drug volume. Model predictions are less accurate in the sparsely sampled regime above 30% release, and future work should include more training data in this region.

A soft implantable drug-delivery platform that enables controlled release of multiple agents

Modulation of physiological pH

Manufacturing. A single-pour lost wax casting technique was used (Figure S1A). The actuation element was composed of high stiffness (Smooth-Sil 950) and low stiffness (Ecoflex 00-20) silicone to enable unidirectional actuation expansion. The self-sealing membrane (Ecoflex 00-20) with a reservoir volume of 13 μL was pre-stretched to varying strains (0%–75%) using a custom rig, and a pore was created using a hypodermic needle (0.24 mm) (Figure S1B). The membrane was then relaxed and bonded to the drug reservoir with a silicone adhesive (Sil-Poxy).

Release measurement. HCl (1 M) or NaOH (1 M) were loaded into the device. Devices were submerged in water and actuated above their activation pressure (133 mmHg). Release was quantified by a pH probe (224 Conductivity TDS Meter) and universal indicator (Innovating Science IS30003).

Controlled release of multiple agents

Manufacturing. A single-pour lost wax casting technique was used (Figure S1A). The actuation element was composed of high stiffness (Smooth-Sil 950) and low stiffness (Ecoflex 00-20) silicone to enable unidirectional actuation expansion. The self-sealing membrane (Ecoflex 00-20) with a reservoir volume of 13 μL was pre-stretched to varying strains (0%, 50%, or 150%) using a custom rig, and a pore was created using a hypodermic needle (small, 0.1842 mm; large, 4.191 mm) (Figure S1B). The membrane was then relaxed and bonded to the drug reservoir with a silicone adhesive (Sil-Poxy).

Activation pressure. Devices were actuated via volume-controlled actuation using a syringe pump (PhD Ultra, Harvard Apparatus) at a constant infusion rate while pressure was measured (Wireless Pressure Sensor, PASCO), and a time-synchronized video was recorded. Opening was determined by slow-motion visual inspection of the video.

Integration of BEI with a soft robotic device

Preparation of the bioadhesive interface and the electrically conductive bioadhesive interface

To prepare the bioadhesive interface, 7 g of poly(vinyl alcohol) (PVA, M_w = 146,000–186,000, ≥99% hydrolyzed) was added into 58 g of deionized water and stirred in a 90°C water bath until completely dissolved. Thirty-five grams of acrylic acid (AAc), 0.2 g of α-ketoglutaric acid, and 0.05 g of *N*,*N*′-bis(acryloyl) cystamine was added to PVA solution equipped with a stirrer. Next, 30 mg of AAc-NHS (*N*-hydroxysuccinimide) was dissolved for every 1 mL of the above solution and then degassed to remove air bubbles. A glass mold was treated with a hydrophobic coating (Rain-X) and equipped with 150-μm spacers. The hydrogel precursor was then poured onto the glass mold, clamped to form a seal, and cured in a UV chamber (365 nm, 10 W power) for 30 min. Immediately after curing, the hydrogel adhesive was spin-coated with polyurethane (PU) solution and stretched to a length and width equal to its equilibrium swelling ratio, as previously reported.[19] The preparation of electrically conductive bioadhesive interface follows the method reported previously.[10]

To prepare the electrically conductive bioadhesive (e-bioadhesive) interface, PVA solution (20 w/w%, ≥99% hydrolyzed, M_w 89,000–98,000) and graphene oxide (GO) solution (Graphene Supermarket) were mixed in a volume ratio of 1:1 and stirred for 48 h to obtain a homogeneous GO-PVA solution. The GO-PVA solution was poured into a glass mold, followed by freezing at −20°C for 8 h and thawing at 25°C for 3 h to form a GO-PVA hydrogel. The GO-PVA hydrogel was further dried in the incubator at 37°C for 1 h and annealed at 100°C for 1 h to obtain the dry GO-PVA film (23.7 w/w% GO). The dry-annealed GO-PVA film was further reduced into reduced GO (rGO)-PVA by immersing in $Na_2S_2O_4$ (0.15 mol/L) and NaOH (0.5 mol/L) solution at 65°C for 1 h, followed by rinsing and immersing in deionized water for 4 h three times to thoroughly remove the residual $Na_2S_2O_4$ and NaOH. The rGO-PVA film was immersed in an aqueous AAc solution (30 w/w% acrylic acid, 0.03 w/w% *N*,*N*′-bis(acryloyl)cystamine, and 0.15 w/w% 2,2′-azobis(2-methylpropionamidine) dihydrochloride in deionized water) for 2 h. The soaked hydrogel was sealed and heated at 70°C for 30 min to form the poly(acrylic acid) (PAA) network, followed by drying on a glass substrate (to ensure constrained drying) under nitrogen flow. To introduce NHS ester groups to the PAA network, the dry film was immersed in an aqueous solution of 1-ethyl-3-(3-dimethylaminopropyl)carbodiimide (0.5 w/w%) and *N*-hydroxysulfosuccinimide sodium salt (sulfo-NHS, 0.25 w/w%) for 5 min at room temperature, providing the as-prepared rGO-PVA-PAA-NHS hydrogel, as previously reported.[10]

Assembly of PU-based device with the bioadhesive interface and the e-bioadhesive electrodes

To assemble e-bioadhesive electrodes, gold foils (20 μm thick, Goodfellow) were first functionalized with primary amine group and assembled with the e-bioadhesive interface.[10] The bioadhesive electrodes were then cut with a 6-mm-diameter biopsy punch and connected with electrode lead wires (AS633, Cooner Wire). The PU-based devices were thoroughly washed with isopropyl alcohol and dried with nitrogen flow, then treated with oxygen plasma for 3 min (30 W power, Harrick Plasma) to increase the hydrophilicity of the surface. The devices were dip-coated with a layer of hydrophilic PU solution (5 w/w%, in 95 w/w% EtOH), followed by placing onto the dried bioadhesive interface and bioadhesive electrodes (Figure S4).

In vivo studies in a rodent model

All studies were conducted according to protocol no. 0118-006-21 approved by the Massachusetts Institute of Technology (MIT) Institutional Animal Care and Use Committee (IACUC). Procedures were carried out at MIT. Protocol reviews were conducted in accordance with the standards outlined in the National Research Council's Guide for the Care and Use of Laboratory Animals and MIT's Animal Welfare Assurance. A total of 12 female Sprague-Dawley rats (250–300 g, The Jackson Laboratory) were used during the development and testing of our SmartSleeve technology. Different subsets of subjects were used for the experimental investigations reported; not all subjects were used in every experimental investigation.

Surgical procedure

For systemic delivery studies, rats were anesthetized using isoflurane (1%–3% in oxygen). A tail-vein catheter was inserted to enable systemic i.v. drug delivery. For amiodarone delivery, 0.5 mg of amiodarone (50 mg/mL) was delivered in a 100-μL bolus, followed by 200 μL of saline.

For epicardial delivery studies, rats were anesthetized using isoflurane (1%–3% in oxygen). Endotracheal intubation was performed, and animals were maintained on a mechanical ventilator (SAR 830P, Harvard Apparatus). The chest cavity was accessed through midline sternotomy, and the pericardium was removed to expose the epicardial surface. Prior to surgery, devices were loaded with 10 μL of amiodarone (50 mg/mL). Devices were placed directly in contact with the epicardial surface and held in place for approximately 10 s to confirm adhesion. Following successful device placement, ECG data were continuously collected via the device. Devices were actuated at 5 psi to deliver 0.5 mg of amiodarone with expected dosing predicted from previous device characterization studies. To trigger on-demand drug delivery in response to decreasing heart rate, glycopyrrolate was delivered via i.v. bolus injection through the tail vein (0.07 mg in 350 μL). The device was triggered after sensing a 25% decrease in RR interval following i.v. administration of glycopyrrolate.

Data acquisition

The electrode sensors and instrumentation data were input into a PowerLab 35 series (PL3516, AD Instruments) high-performance data-acquisition system with a 1,000 Hz sampling frequency. During the experiments, data were monitored live via LabChart software (AD Instruments). After the experiments, data were exported into and processed in MATLAB (MathWorks).

Control system design and instrumentation

Our group has built a custom electropneumatic control system utilizing electropneumatic pressure regulators and valves (SMC Pneumatics, SMC) controlled by custom software described previously.[20] The software is designed to allow custom pressure waveforms to be input. To implement ECG-informed on-demand drug delivery in our system, we monitored live RR intervals via LabChart software using the ECG analysis add-on package (AD Instruments). We used this measurement to trigger device actuation via our custom control system following a 25% decrease in RR interval, with baseline RR interval measured as the average RR interval for 10 s prior to intervention (i.v. administration of glycopyrrolate).

In vivo studies in a porcine model

All studies were conducted according to protocol no. 0118-006-21 approved by the MIT IACUC. Procedures were carried out at MIT. Protocol reviews were conducted in accordance with the standards outlined in the National Research Council's Guide for the Care and Use of Laboratory Animals and MIT's Animal Welfare Assurance. Female Yorkshire (30–40 kg) swine were sourced from Parson's Farm (Hadley, MA, USA). A total of four swine were used during the development and testing of our system. Different subsets of subjects were used for the experimental investigations reported; not all subjects were used in every experimental investigation. Animals were acclimated and cared for according to standard facility protocols. Each experiment was conducted under 2%–3% isoflurane anesthesia, titrated to each animal to maintain a stable anesthetic plane. Anesthesia and mechanical ventilation were controlled through an Aestiva 5 Anesthesia Machine (GE Datex Ohmeda). Vital signs were monitored via a Cardell Veterinary Monitor Max 1. After completing each study and acquiring the data, animals were euthanized using Fatal-Plus solution (Vortech Pharmaceuticals) at a dose of 110 mg/kg body weight.

Surgical procedure

After induction of anesthesia, the animal was intubated and placed on mechanical ventilation. A transesophageal electrocardiogram catheter was placed to monitor the heart rate. A carotid arterial sheath and jugular venous line were placed using cut-down technique for animal systemic drug administration. A Foley catheter was placed for urine output monitoring. The chest cavity was accessed through midline sternotomy. The pericardium was opened to allow exposure of the epicardial surface. The epicardial surface was washed with saline to ensure good adherence. Prior to surgery, devices were loaded with 400 μL or 300 μL of epinephrine (1 mg/mL). Devices were placed directly in contact with the epicardial surface and held in place for approximately 10 s to confirm adhesion. Following successful device placement, ECG data were continuously collected via the device. Devices were actuated to deliver epinephrine at dose 1 (~0.32 mg) or dose 2 (~0.08 mg) with expected dosing predicted using the Gaussian process regressor (Figure S7) based on the actuation regime (actuation pressure 0.75–1.5 psi) and device parameters (loading volume, opening pressure). To generate an ECG signal that could be used to trigger on-demand drug delivery, the heart was externally paced to 120 bpm. To do so, an epicardial pacing wire was sutured to the right atrium and connected to a temporary external pacemaker (Medtronic). After pacing was stopped, the device was triggered after sensing a return to baseline heart rate prior to initiation of pacing.

Data acquisition

We used the same data-acquisition system as described above for our rodent studies.

Control system design and instrumentation

We used the same custom control system as described above for our rodent studies. To implement ECG-informed on-demand drug delivery in our system, we monitored live heart rate via LabChart software using the ECG analysis add-on package (AD Instruments). We measured baseline heart rate as the average heart rate for 10 s prior to intervention (initiation of pacing). We used this measurement as the threshold for "return to baseline" after pacing that was used to trigger device actuation via the custom control system described previously.

Closed-loop control of drug delivery

To implement ECG-informed closed-loop on-demand drug delivery, we monitored a single-lead ECG (lead I) from a patient simulator (FS410 ECG Simulator, FLUKE Biomedical) via LabChart software using the ECG analysis add-on package (AD Instruments). RR interval was calculated from the ECG signal. To generate a change in RR interval, heart rate of the patient simulator was varied from 60 bpm to 120 bpm back to 60 bpm. A custom "Event" was created in LabChart that would send a trigger pulse to the custom pneumatic control system each time the RR interval passed 0.8 s. When the event was sensed (trigger 1: change from 60 bpm to 100 bpm; trigger 2: change from 120 bpm to 60 bpm), LabChart sent a pulse to the control system, triggering device actuation and drug delivery.

SUPPLEMENTAL INFORMATION

Supplemental information can be found online at https://doi.org/10.1016/j.device.2024.100419.

ACKNOWLEDGMENTS

The authors would like to acknowledge Mossab Y. Saeed for his surgical expertise during the porcine procedures and the support of the Division of Comparative Medicine staff at MIT for the care and monitoring of our animals during surgical procedures. The data were analyzed and graphed using Prism10 (GraphPad). K.L.M. and E.T.R. acknowledge funding from the Institute for Medical Engineering and Science and the Mechanical Engineering Department at MIT. X.Z. acknowledges funding from the National Institutes of Health (grant nos. 1R01HL153857-01 and 1R01HL167947-01), the National Science Foundation (grant no. EFMA-1935291), and Department of Defense Congressionally Directed Medical Research Programs (grant no. PR200524P1).

AUTHOR CONTRIBUTIONS

K.L.M. and E.T.R. conceptualized the work. K.L.M, E.T.R., X.Z., C.E.V., J.B., and W.W. designed the experiments. J.D., H.Y., and X.Z. contributed materials for the experiments. K.L.M, C.V., J.B., and W.W. conducted the experiments. K.L.M, J.B., and E.T.R. analyzed the results. K.L.M, J.B., B.A., and E.T.R. wrote the manuscript.

DECLARATION OF INTERESTS

H.Y. and X.Z. are inventors of a patent application (US patent 62/845,976) that covers the dry-crosslinking mechanism and the design of the tissue

Please cite this article in press as: Mendez et al., SmartSleeve: A sutureless, soft robotic epicardial device that enables switchable on-off drug delivery in response to epicardial ECG sensing, Device (2024), https://doi.org/10.1016/j.device.2024.100419

bioadhesive. H.Y. and X.Z. have a financial interest in SanaHeal, Inc., a biotechnology company focused on the development of bioadhesive technologies. X.Z. has a financial interest in SonoLogi and Magnendo. E.T.R. serves on the board of directors for Affluent Medical as well as the board of advisors for Pumpinheart and Helios Cardio. E.T.R. is an academic co-founder of Fada Medical and Spheric Bio.

Received: February 12, 2024
Revised: April 6, 2024
Accepted: May 14, 2024
Published: September 20, 2024

REFERENCES

1. Maslov, M.Y., Edelman, E.R., Wei, A.E., Pezone, M.J., and Lovich, M.A. (2013). High concentrations of drug in target tissues following local controlled release are utilized for both drug distribution and biologic effect: An example with epicardial inotropic drug delivery. J. Contr. Release *171*, 201–207. https://doi.org/10.1016/j.jconrel.2013.06.038.
2. Maslov, M.Y., Edelman, E.R., Pezone, M.J., Wei, A.E., Wakim, M.G., Murray, M.R., Tsukada, H., Gerogiannis, I.S., Groothuis, A., and Lovich, M.A. (2014). Myocardial drug distribution generated from local epicardial application: Potential impact of cardiac capillary perfusion in a swine model using epinephrine. J. Contr. Release *194*, 257–265. https://doi.org/10.1016/j.jconrel.2014.09.012.
3. Bolderman, R.W., Hermans, J.J.R., Rademakers, L.M., de Jong, M.M.J., Bruin, P., Dias, A.A., van der Veen, F.H., and Maessen, J.G. (2011). Epicardial application of an amiodarone-releasing hydrogel to suppress atrial tachyarrhythmias. Int. J. Cardiol. *149*, 341–346. https://doi.org/10.1016/j.ijcard.2010.02.014.
4. SIDEN, R., Flowers, W.E., and Levy, R.J. (1992). Epicardial propranolol administration for ventricular arrhythmias in dogs: matrix formulation and characterization. Biomaterials *13*, 764–770. https://doi.org/10.1016/0142-9612(92)90015-G.
5. Labhasetwar, V., Kadish, A., Underwood, T., Sirinek, M., and Levy, R.J. (1993). The efficacy of controlled release D-sotalol-polyurethane epicardial implants for ventricular arrhythmias due to acute ischemia in dogs. J. Contr. Release *23*, 75–85. https://doi.org/10.1016/0168-3659(93)90072-D.
6. Labhasetwar, V., Underwood, T., Gallagher, M., Murphy, G., Langberg, J., and Levy, R.J. (1994). Sotalol Controlled-Release Systems for Arrhythmias: In Vitro Characterization, in Vivo Drug Disposition, and Electrophysiologic Effects. J. Pharmaceut. Sci. *83*, 156–164. https://doi.org/10.1002/jps.2600830209.
7. Josephson, M.E. (2008). Clinical Cardiac Electrophysiology : Techniques and Interpretations, 4th ed. (Lippincott Williams & Wilkins).
8. Somani, S., Russak, A.J., Richter, F., Zhao, S., Vaid, A., Chaudhry, F., De Freitas, J.K., Naik, N., Miotto, R., Nadkarni, G.N., et al. (2021). Deep learning and the electrocardiogram: review of the current state-of-the-art. Europace *23*, 1179–1191. https://doi.org/10.1093/europace/euaa377.
9. Siontis, K.C., Noseworthy, P.A., Attia, Z.I., and Friedman, P.A. (2021). Artificial intelligence-enhanced electrocardiography in cardiovascular disease management. Nat. Rev. Cardiol. *18*, 465–478. https://doi.org/10.1038/s41569-020-00503-2.
10. Deng, J., Yuk, H., Wu, J., Varela, C.E., Chen, X., Roche, E.T., Guo, C.F., and Zhao, X. (2021). Electrical bioadhesive interface for bioelectronics. Nat. Mater. *20*, 229–236. https://doi.org/10.1038/s41563-020-00814-2.
11. Whyte, W., Roche, E.T., Varela, C.E., Mendez, K., Islam, S., O'Neill, H., Weafer, F., Shirazi, R.N., Weaver, J.C., Vasilyev, N.V., et al. (2018). Sustained release of targeted cardiac therapy with a replenishable implanted epicardial reservoir. Nat. Biomed. Eng. *2*, 416–428. https://doi.org/10.1038/s41551-018-0247-5.
12. Varela, C.E., Monahan, D.S., Islam, S., Whyte, W., Bonnemain, J., Ngoy, S., Fisch, S., Duffy, G.P., and Roche, E.T. (2022). Epicardial reservoir-enabled multidose delivery of exogenous FSTL1 leads to improved cardiac function, healing, and angiogenesis. Preprint at bioRxiv. https://doi.org/10.1101/2022.11.02.513725.
13. Hu, L., Bonnemain, J., Saeed, M.Y., Singh, M., Quevedo Moreno, D., Vasilyev, N.V., and Roche, E.T. (2023). An implantable soft robotic ventilator augments inspiration in a pig model of respiratory insufficiency. Nat. Biomed. Eng. *7*, 110–123. https://doi.org/10.1038/s41551-022-00971-6.
14. Mendez, K., Whyte, W., Freedman, B.R., Fan, Y., Varela, C.E., Singh, M., Cintron-Cruz, J.C., Rothenbücher, S.E., Li, J., Mooney, D.J., and Roche, E.T. (2023). Mechanoresponsive Drug Release from a Flexible, Tissue-Adherent, Hybrid Hydrogel Actuator. Adv. Mater., e2303301. https://doi.org/10.1002/adma.202303301.
15. Das, R., and Yoo, H. (2015). Biotelemetry and Wireless Powering for Leadless Pacemaker Systems. IEEE Microw. Wireless Compon. Lett. *25*, 262–264. https://doi.org/10.1109/LMWC.2015.2400920.
16. Pya, Y., and Abdiorazova, A. (2021). Elimination of drive exit line: transcutaneous energy transmission. Ann. Cardiothorac. Surg. *10*, 393–395. https://doi.org/10.21037/acs-2020-cfmcs-200.
17. Rotariu, C., Manta, V., and Costin, H. (2012). Wireless remote monitoring system for patients with cardiac pacemakers. In 2012 International Conference and Exposition on Electrical and Power Engineering (IEEE), pp. 845–848. https://doi.org/10.1109/ICEPE.2012.6463828.
18. Walser, E.M. (2012). Venous Access Ports: Indications, Implantation Technique, Follow-Up, and Complications. Cardiovasc. Intervent. Radiol. *35*, 751–764. https://doi.org/10.1007/s00270-011-0271-2.
19. Wu, J., Yuk, H., Sarrafian, T.L., Guo, C.F., Griffiths, L.G., Nabzdyk, C.S., and Zhao, X. (2022). An off-the-shelf bioadhesive patch for sutureless repair of gastrointestinal defects. Sci. Transl. Med. *14*, eabh2857. https://doi.org/10.1126/scitranslmed.abh2857.
20. Horvath, M.A., Hu, L., Mueller, T., Hochstein, J., Rosalia, L., Hibbert, K.A., Hardin, C.C., and Roche, E.T. (2020). An organosynthetic soft robotic respiratory simulator. APL Bioeng. *4*, 026108. https://doi.org/10.1063/1.5140760.

DEVICE, Volume *2*

Supplemental information

SmartSleeve: A sutureless, soft robotic epicardial device that enables switchable on-off drug delivery in response to epicardial ECG sensing

Keegan L. Mendez, Claudia E. Varela, Jean Bonnemain, Jue Deng, Hyunwoo Yuk, Brian Ayers, William Whyte, Xuanhe Zhao, and Ellen T. Roche

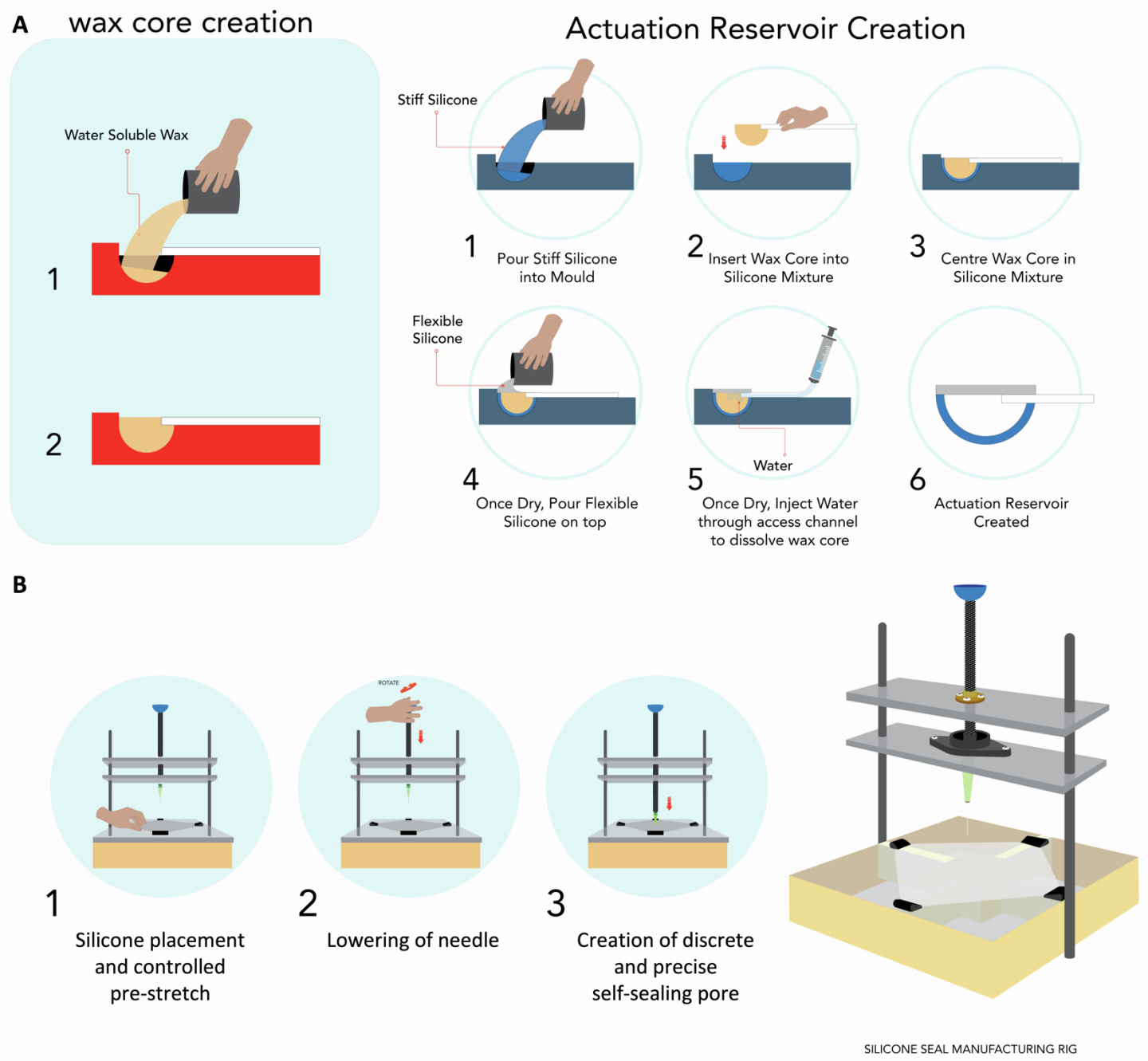

Figure S1. SoftSwitch Manufacturing. (A) Manufacturing of a unidirectional actuation reservoir. The actuation element is composed of high stiffness (Smooth-Sil 950) and low stiffness (Ecoflex 00-20) silicone to enable unidirectional expansion on actuation. A single-pour lost wax casting technique is used to create the actuation reservoir. A water-soluble wax core is created (left). The wax core is then used to create the silicone actuation reservoir (right). High stiffness silicone is poured into the device mold. The wax core is centered in the silicone and allowed to partially cure. The low stiffness silicone is poured, and the device is cured overnight. Water is used to dissolve the wax core, resulting in a two-stiffness actuation reservoir that expands in one direction when pressurized. (B) Manufacturing of a self-sealing silicone pore. The self-sealing membrane (Ecoflex 00-20) is created using a custom rig to pre-stretch the membrane to varying strains and create a single pore using a hypodermic needle. The membrane is placed in the rig and stretched to known strain. The needle is lowered to create a discrete and precise self-sealing pore. The membrane is then relaxed and bonded to the actuation reservoir.

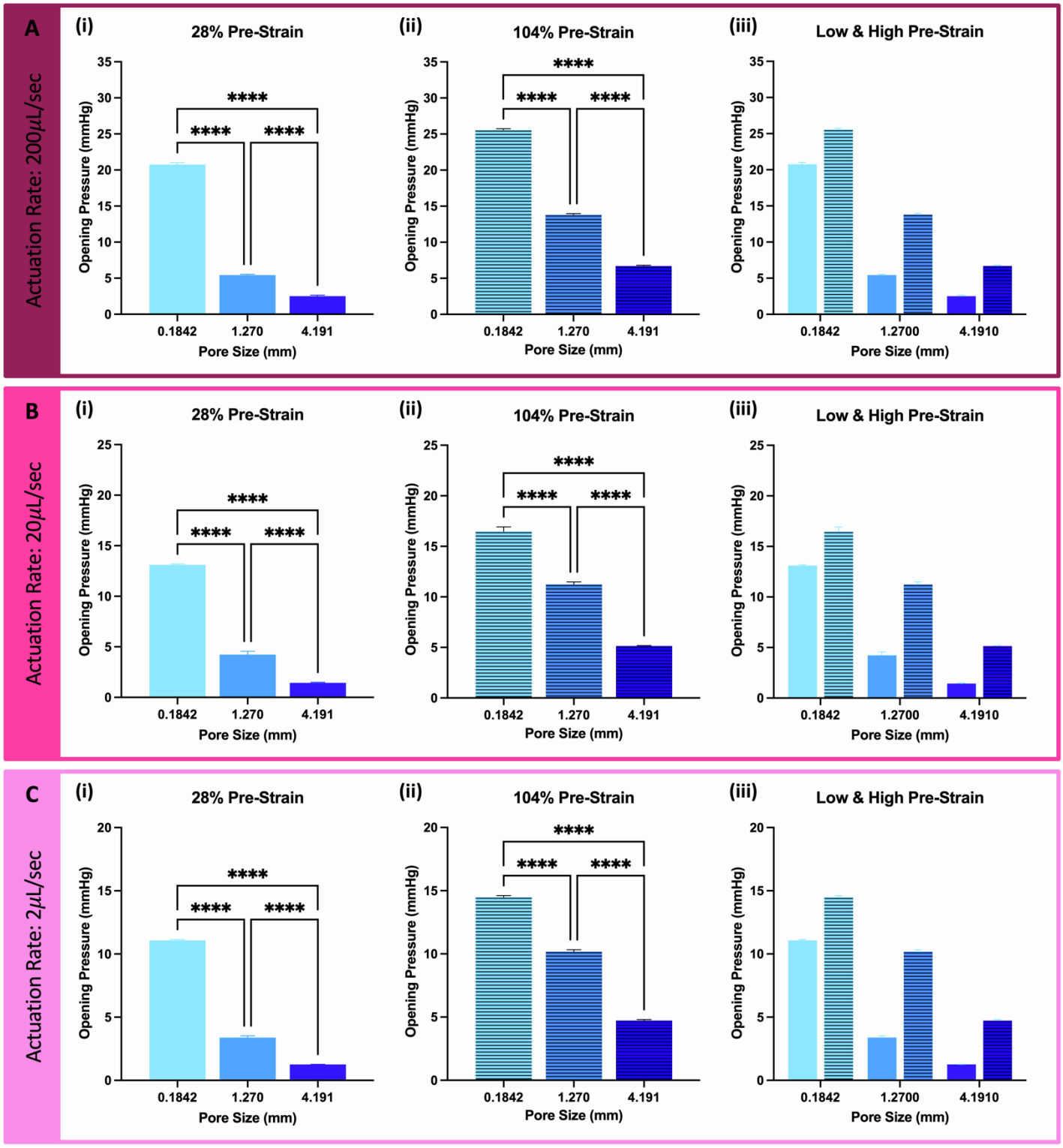

Figure S2. Effect of pore size on switch activation pressure. The effect of pore size on opening pressure at (A) fast actuation rate (200μL/sec), (B) medium actuation rate (20μL/sec), and (C) slow actuation rate (2μL/sec) with (A-C) (i) low membrane pre-strain (28%), (ii) high membrane pre-strain (104%), and (iii) low and high membrane pre-strain (n=3 devices per group; 5 activations per device). * P<0.0332, ** P<0.0021, *** P<0.0002, **** P<0.0001; ordinary one-way ANOVA with Tukey's multiple comparison test within each pre-strain group. (A-C) (iii) For all actuation rates, opening pressure decreases with increasing pore size and increases with increasing membrane pre-strain.

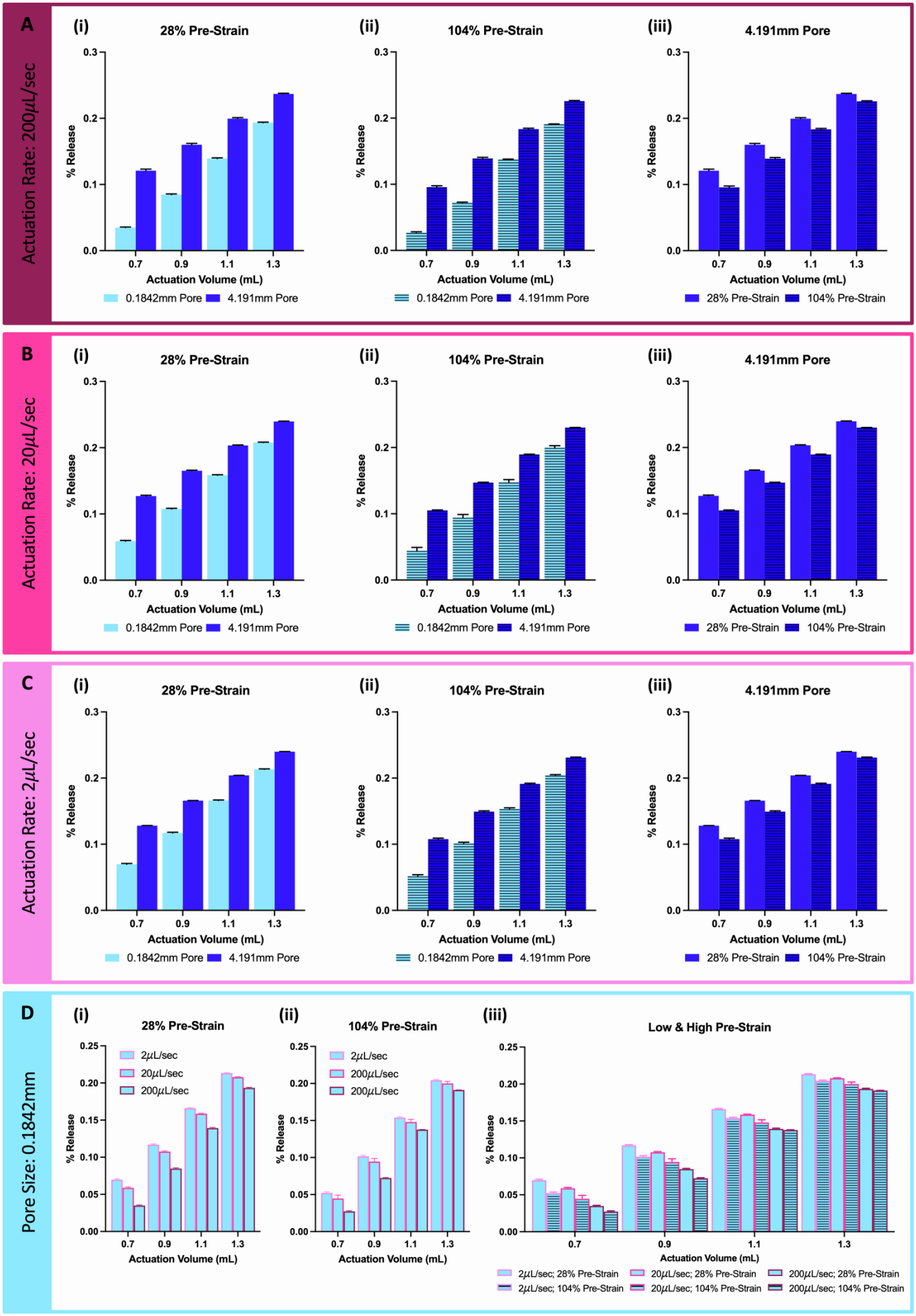
A
Actuation Rate: 200μL/sec
(i)
28% Pre-Strain
(ii)
104% Pre-Strain
(iii)
4.191mm Pore
% Release
Actuation Volume (mL)
0.1842mm Pore
4.191mm Pore
28% Pre-Strain
104% Pre-Strain
B
Actuation Rate: 20μL/sec
C
Actuation Rate: 2μL/sec
D
Pore Size: 0.1842mm
2μL/sec
20μL/sec
200μL/sec
Low & High Pre-Strain
2μL/sec; 28% Pre-Strain
20μL/sec; 28% Pre-Strain
200μL/sec; 28% Pre-Strain
2μL/sec; 104% Pre-Strain
20μL/sec; 104% Pre-Strain
200μL/sec; 104% Pre-Strain

Figure S3. Effect of pre-strain and pore size on percent release. The effect of pre-strain and pore size on percent release at (A) fast actuation rate (200μL/sec), (B) medium actuation rate (20μL/sec), and (C) slow actuation rate (2μL/sec) (n=3 devices per group). (A-C) (i) low membrane pre-strain (28%) for small pore size (0.1842mm) and large pore size (4.191mm), (ii) high membrane pre-strain (104%) for small pore size (0.1842mm) and large pore size (4.191mm), and (iii) low and high membrane pre-strain for large pore size (4.191mm) (n=3 devices per group). (D) The effect of actuation rate on percent release for small pore size (0.1842mm) at (i) low membrane pre-strain (28%), (ii) high membrane pre-strain (104%), and (iii) low and high membrane pre-strain (n=3 devices per group). For all actuation rates, percent release increases with increasing actuation volume (indirect measure of pressure). For a given actuation volume, percent release decreases with increasing actuation rate. For a given volume and actuation rate, percent release decreases with increasing pre-strain and increases with increasing pore size.

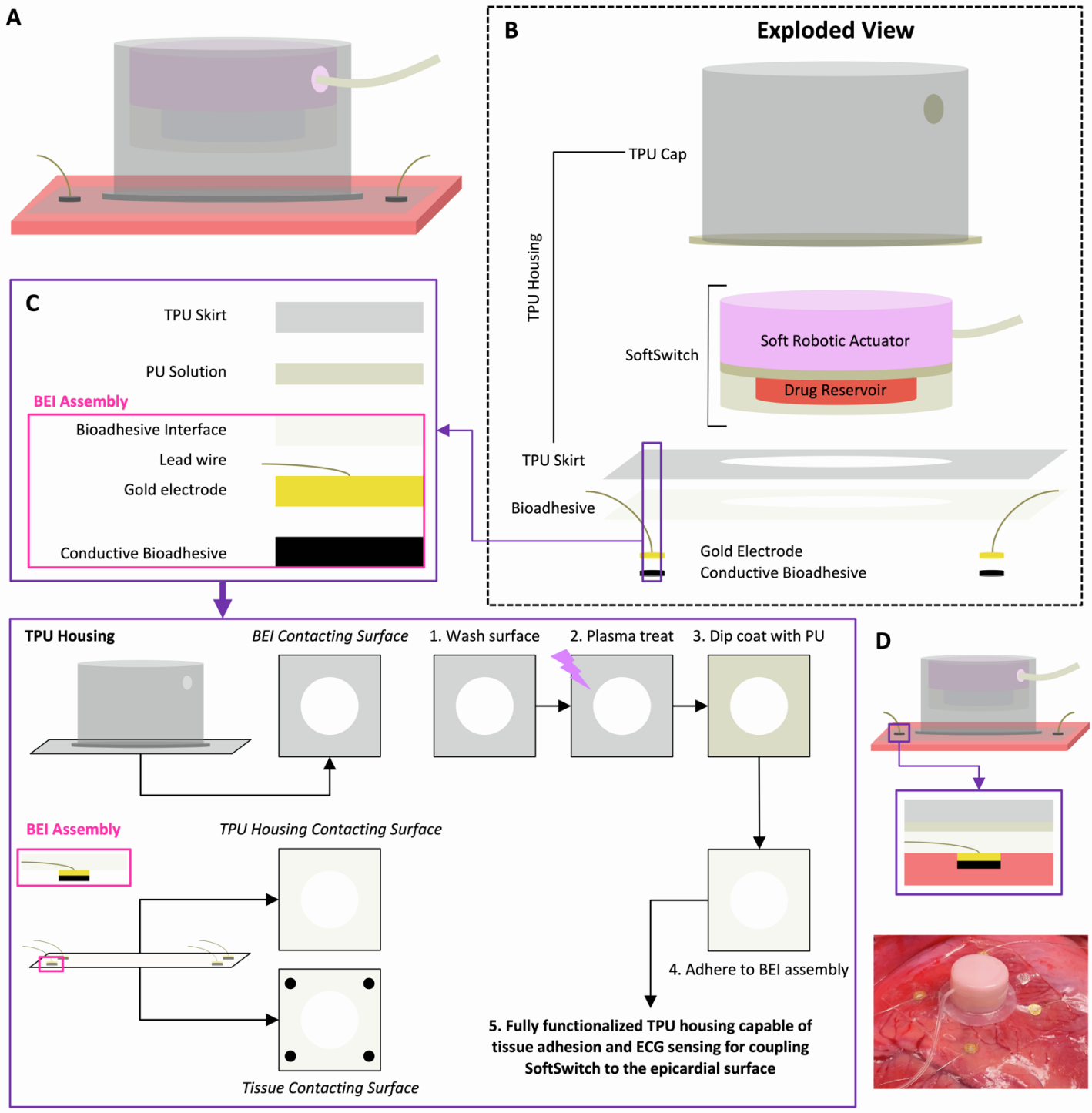

Figure S4. Manufacturing of functionalized TPU housing. (A) Schematic of SmartSleeve coupled to epicardial surface. (B) SmartSleeve consists of a soft robotic drug delivery device, SoftSwitch, composed of a soft robotic actuator and a self-sealing drug reservoir, that is coupled to a bioadhesive electronic interface (BEI) via a thermoplastic polyurethane (TPU) housing. (C) Coupling of TPU housing and BEI assembly. TPU housing is coupled with the BEI assembly via plasma treatment and a polyurethane layer. (D) Schematic (top) and in vivo demonstration (bottom) of fully functionalized TPU housing that enables tissue adhesion and ECG sensing at the epicardial surface.

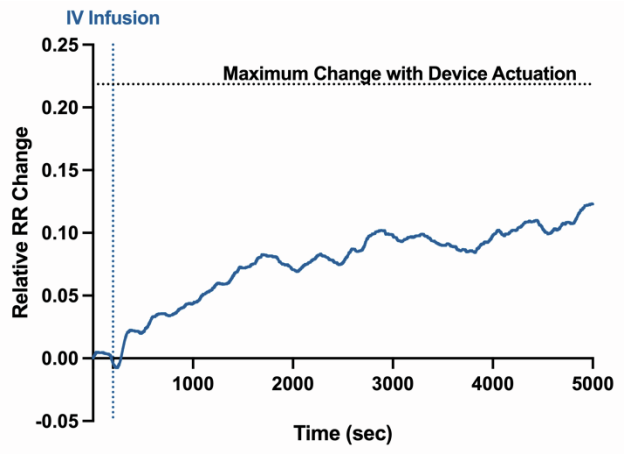

Figure S5. Systemic vs. device-enabled epicardial delivery of amiodarone in a rodent model. Relative RR change following systemic delivery of amiodarone via tail vein infusion. Dashed horizontal line indicates maximum relative RR change achieved by device actuation resulting in epicardial delivery of the same dose. Device-enabled epicardial delivery results in a larger physiological response than could be achieved by systemic delivery of the same dose after 5000 seconds.

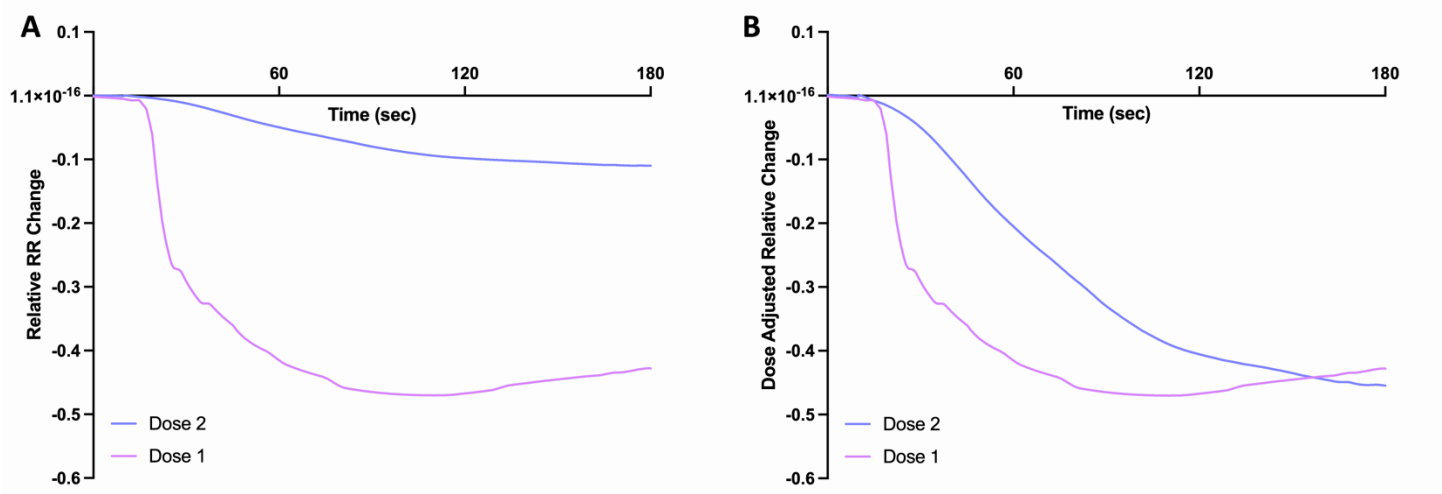

Figure S6. Dose-adjusted epicardial delivery of epinephrine in a porcine model. (A) Relative RR change following epicardial delivery of two different doses of epinephrine (Dose 1 = 4x Dose 2; both doses administered in the same pig). (B) Dose-adjusted relative RR change. Maximum dose-adjusted relative RR similar for both doses. Dose 1 reaches maximum effect more rapidly than Dose 2.

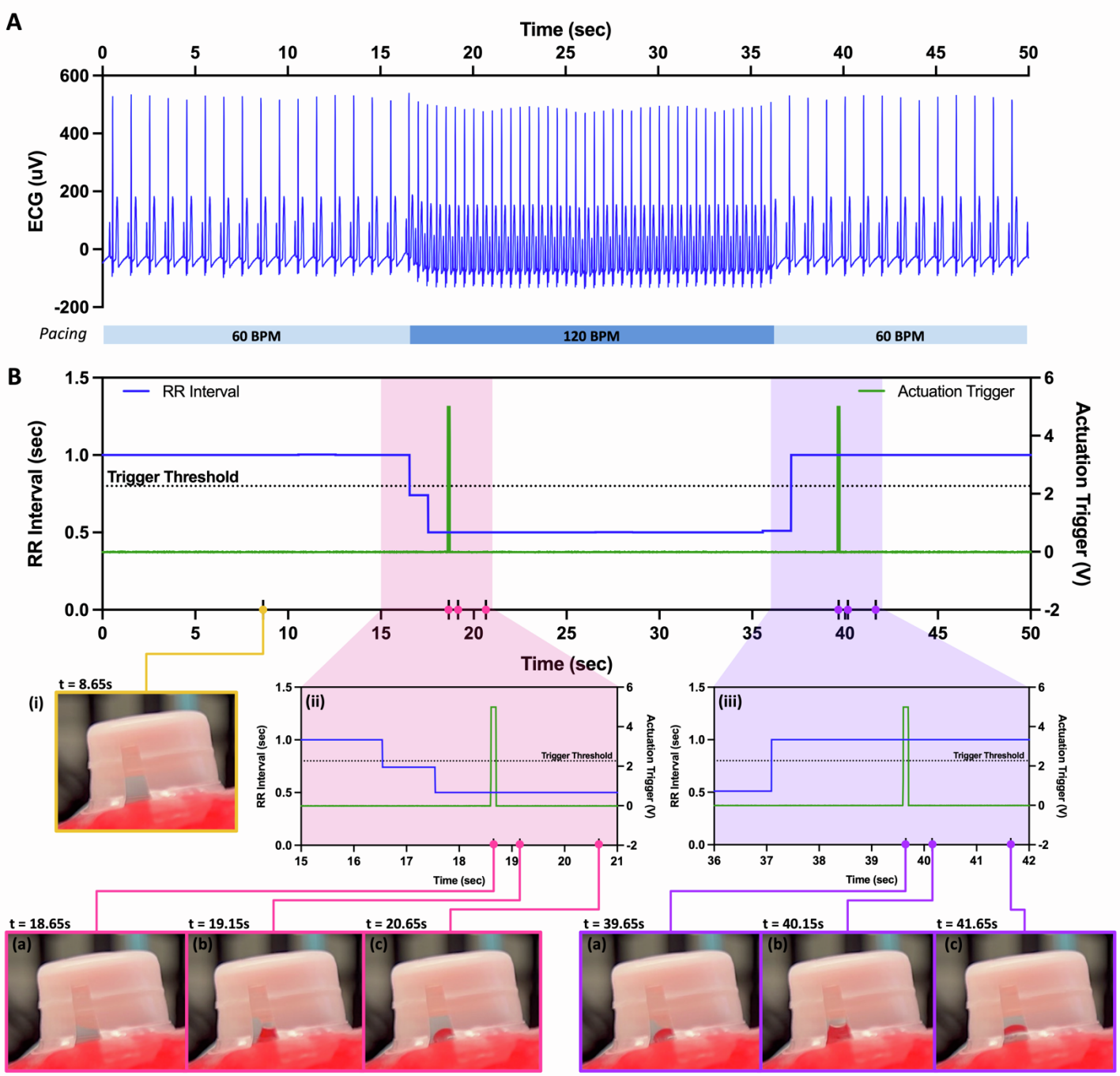

Figure S7. Closed-loop control of drug delivery in response to real-time ECG signal. (A) Input ECG signal from single lead of patient simulator. Heart rate was varied from 60BPM to 120BPM and then back to 60BPM. (B) RR interval (left y-axis; blue) calculated from ECG signal in (A) and actuation trigger (right y-axis; green) corresponding to automatic pulse sent to custom control box for device actuation after sensing trigger threshold event (RR interval = 0.8 sec). Filled circles on x-axis correspond to timepoints of device photos. (i) Device prior to actuation (t = 8.65 sec). No evidence of drug release prior to sensing threshold signal. (ii) Closed-loop device actuation after sensing trigger threshold event (RR interval < 0.8 sec) (t = 15-21 sec). (i)(a) device actuation and (i)(b-c) drug release following automated pulse sent to control box. (iii) Closed-loop device actuation after sensing trigger threshold event (RR interval > 0.8 sec) (t = 36-42 sec). (ii)(a) device actuation and (ii)(b-c) drug release following automated pulse sent to control box.

A

Model Type	Results
Gaussian Process Regression	RMSE: 0.488
Kernel Function: Matern 5/2	R-Squared: 0.99
Bias Function: Constant	MSE: 0.238
Fit Method: Exact	MAE: 0.190
Active Set Method: Random	Prediction speed ~23000 obs/sec
Optimizer: Quasinewton	Training time 0.51688 sec
Number of Observations: 152	
5-fold Cross Validation	

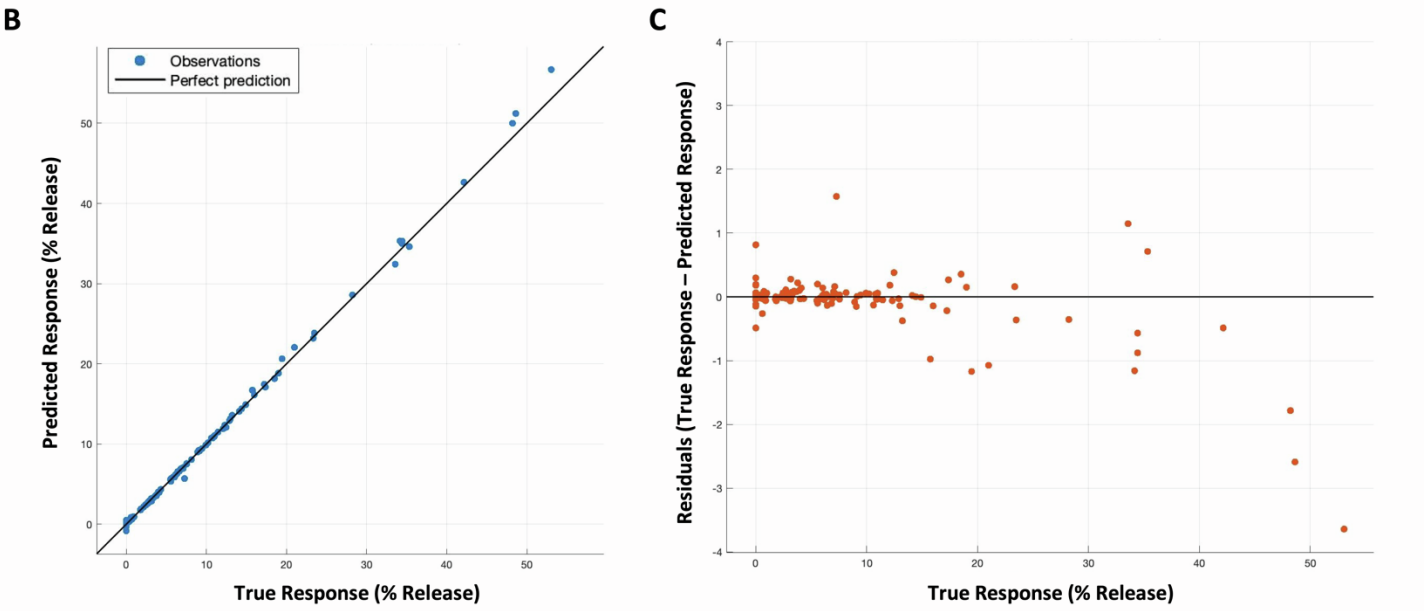

Figure S8. Gaussian process regressor used to predict drug release. (A) To build a predictive model for drug release profile, MATLAB Regression Learner toolbox was used to automatically assess a set of supervised machine learning algorithms. Candidate regression models were trained and evaluated by applying five-fold cross validation, then ranked according to root mean square error (RMSE). The top-performing model, a Gaussian process regressor (Results: RMSE = 0.488; R-Squared = 0.99; MSE = 0.238; MAE = 0.190) was subsequently used to predict the output drug release (% Release) as a function of the device manufacturing parameters (pore size, membrane pre-strain, drug loading volume) and the device actuation parameters (actuation volume, actuation pressure, number of prior actuations). (B) Predicted Response vs. True Response for the Gaussian process regressor. (C) Residuals vs. True Response for the Gaussian process regressor.